# Effect of overlapping double layers and pH on electrokinetics in a microchannel

A Dissertation Presented

by

**Ardavan Mansourpour**

Supervisors

**Dr. Vahid Joekar-Niasar**

**Prof. Ruud Schotting**

Department of Earth Sciences

University of Utrecht

Master of Science

August 2013

# Effect of overlapping double layers and pH on electrokinetics in a microchannel

A Dissertation Presented

by

Ardavan Mansourpour

# Electrokinetics in microchannels

## ACKNOWLEDGMENTS

It is a pleasure to thank those people who gave continuous encouragement, help and assistance during the completion of this study.

First of all, I express my gratitude to dear Dr. Vahid Joekar-Niasar for his encouragements, valuable time, advice, and comments to me to take on this big challenge. Without his intellectual advice and support, I would think this study would not be completed.

I also would like to thank Professor Ruud Schotting for his support and help. It was a pleasure for me to have the opportunity of being his student.

I especially thank my parents, who have always been a big support in my life. And, last but not least, I would like to thank the love and hope of my life, my dear Samira for standing by me, supporting me, and giving me the courage to overcome the problems.

## ABSTRACT

Electroosmosis in porous media has a very wide range of applications such as soil remediation, oil recovery, subsurface exploration, drug delivery in tissues. In this research, we focus on solving Poisson-Boltzmann equation in a rectangular channel with different boundary, geometrical and pH conditions in order to capture the effective factors in electroosmotic flow (EOF) in a microchannel.
Based on the results, the electroosmotic flow varies significantly with overlapping condition of double layers, represented by a scaling factor, which is the ratio of half of the height of a channel to Debye length, referred to as$\overline{K}$. The other factor is the aspect ratio of the channel, which is the ratio of width to the height of the channel. Results show that the effect of thickness of the electric double layer on EOF is crucial, while the aspect ratio was found to have less effect on EOF.

The pH effects were also taken into account as the changes in pH in known to have significant effect on the state of EOF and electroosmotic permeability can change by orders of magnitude. The results show a decline in EO permeability as the pH increases, if the $\overline{K}$ effect on electroosmotic permeability is still important.

As known, the linear Poisson-Boltzmann equation cannot be used for larger zeta potential values as well as constant charge boundary condition. Thus, we showed the effect of ignorance of this nonlinearity for a large zeta potential 100mV. Results show that if a linear Poisson-Boltzmann equation for a large zeta potential condition is used, the electroosmotic permeability will be underestimated and the average electric potential will be overestimated. Moreover, results showed that solving the linear Poisson-Boltzmann equation for constant charge condition would not provide realistic results.

The results of this study not only can be used to understand the fundamentals of electroosmosis in porous media but also will be used for upscaling this phenomenon to Darcy scale using a pore network modeling approach.

# Table of Contents

ACKNOWLEDGMENTS ..... 5

ABSTRACT ..... 6

1. INTRODUCTION ..... 10

1.1. FUNDAMENTALS OF ELECTROKINETICS ..... 11
1.1.1. DEBYE LENGTH ..... 12
1.2. LITERATURE REVIEW AND PREVIOUS STUDIES ..... 14
1.2.1. ELECTROOSMOSIS IN SOIL REMEDIATION ..... 14
1.2.2. IMPORTANT FACTORS IN ELECTROOSMOSIS ..... 15
PH ..... 15
GEOMETRICAL AND PHYSICAL FACTORS ..... 16
OBJECTIVES ..... 19

2. GOVERNING EQUATIONS ..... 20

2.1. POISSON- BOLTZMANN EQUATION ..... 20
2.2. DEBYE LENGTH ..... 22
2.3. THE ELECTROOSMOTIC FLOW ..... 22
2.4. THE HYDRODYNAMIC FLOW ..... 23
2.5. INCLUSION OF PH EFFECTS ON SURFACE CHARGE ..... 24
2.6. NUMERICAL SOLUTION ..... 25
2.6.1. LINEAR PB EQUATION ..... 25
2.6.2. BOUNDARY AND INITIAL CONDITIONS ..... 27
2.6.3. HOMOGENEOUS AND HETEROGENEOUS SURFACES ..... 27
2.6.4. NON-LINEAR PB EQUATION ..... 27

3. NUMERICAL EXAMPLES FOR ELECTRIC FIELD ..... 28

3.1. TWO-DIMENSIONAL EXAMPLE ..... 29
3.2. MODEL VERIFICATION ..... 29
3.3. THREE-DIMENSIONAL EXAMPLE ..... 33
3.3.1. THE EFFECT OF OVERLAPPING AND ASPECT RATIO ..... 34
3.4. AN EXAMPLE OF HETEROGENEOUSLY DISTRIBUTION OF ELECTRIC POTENTIAL ..... 35

4. ELECTROOSMOTIC PERMEABILITY IN A SINGLE CHANNEL ..... 39

**4.1. LINEAR PB EQUATION WITH CONSTANT POTENTIAL BOUNDARY CONDITION ..... 40**
4.1.1. ELECTROOSMOTIC FLOW VS. HYDRODYNAMIC FLOW ..... 43
**4.2. NON-LINEAR PB EQUATION WITH CONSTANT POTENTIAL BOUNDARY ..... 43**
4.2.1. COMPARING THE RESULTS OF LINEAR AND NON-LINEAR MODELS ..... 44
**4.3. NON-LINEAR PB EQUATION WITH CONSTANT CHARGE BOUNDARY ..... 45**
4.3.1. ELECTROOSMOTIC FLOW VS. HYDRODYNAMIC FLOW IN NON-LINEAR PB EQUATION ..... 46
**4.4. PH EFFECTS ON ELECTRIC FIELD AND ELECTROOSMOTIC PERMEABILITY FOR A CONSTANT CHARGE BOUNDARY CONDITION ..... 47**

**5. CONCLUSION ..... 50**

**6. REFERENCES ..... 52**

# List of Figures

FIGURE 1 : HELMHOLTZ AND DIFFUSE ELECTRIC DOUBLE LAYER. (8) ..... 12
FIGURE 2 : A SCHEMATIC DIAGRAM OF THE ALIGNMENT OF IONIC SPECIES WITHIN THE ELECTRIC FIELD DEVELOPED BY THE SOIL SURFACE AND THE PORE FLUID VELOCITY PROFILE GENERATED WHEN AN ELECTRIC FIELD IS APPLIED ALONG THE CAPILLARY NORMAL TO THE DIRECTION OF THE ELECTRIC FIELD OF THE SURFACE. (11) ..... 15
FIGURE 3: SCHEMATIC ILLUSTRATION OF REPRESENTATIVE ELEMENTARY VOLUME (REV): THE LENGTH SCALE OF THE REV IS MUCH LARGER THAN THE PORE SCALE, BUT CONSIDERABLY SMALL (18) ..... 17
FIGURE 4: SCHEMATIC ILLUSTRATION OF EOF IN CHARGED RANDOM POROUS MEDIA.(3) ..... 18
FIGURE 5 : THE ELECTROOSMOTIC PERMEABILITY CHANGING WITH THE BULK IONIC CONCENTRATION. E = 0.38, Z =−50 MV, AND E = $1 \times 10^4$ V/M.(3) ..... 18
FIGURE 6 : ELECTRIC POTENTIAL DISTRIBUTION WHEN $\boldsymbol{Cb}$ IS EQUAL TO (A) 0.0005 MOL/$M^3$ AND (B) 0.05 MOL/$M^3$ ..... 30
FIGURE 7 : DIFFERENCE BETWEEN LINEAR PB NUMERICAL AND ANALYTICAL SOLUTIONS WHEN $\boldsymbol{Cb}$ IS EQUAL TO (A) 0.0005 MOL/$M^3$ AND (B) 0.05 MOL/$M^3$ ..... 31
FIGURE 8: TWO HOMOGENEOUSLY CHARGED SURFACES CONTAINING A NEWTONIAN FLUID. $\boldsymbol{Cb}$ =0.05 MOL/$M^3$ ..... 32
FIGURE 9:TWO HOMOGENEOUSLY CHARGED SURFACES. $\boldsymbol{Cb}$=0.0005 MOL/$M^3$ ..... 32
FIGURE 10 : 2-D DOMAIN WITH HOMOGENEOUSLY CHARGED BOUNDARY. ..... 33
FIGURE 11 : A CROSS-SECTION OF THE ELECTRIC POTENTIAL DISTRIBUTION IN A HETEROGENEOUS DOMAIN ..... 34
FIGURE 12 : THE CROSS SECTION OF THE HOMOGENEOUS DOMAIN WITH OVERLAPPING DIFFUSE DOUBLE-LAYER ..... 36
FIGURE 13 : THE AVERAGE ELECTRIC POTENTIAL IN LENGTH LAYERS OF THE CHANNEL AT DIFFERENT $\boldsymbol{K}$ RATIOS ..... 37
FIGURE 14 : ELECTRIC FIELD IN A LONGITUDINAL CROSS SECTION OF A HETEROGENEOUS CHANNEL ..... 37
FIGURE 15 : THE AVERAGE ELECTRIC POTENTIAL IN LENGTH LAYERS OF THE CHANNEL AT DIFFERENT $\boldsymbol{K}$ RATIOS IN HETEROGENEOUS DOMAIN ..... 38
FIGURE 16 : ELECTROOSMOTIC PERMEABILITY AS A FUNCTION OF $\boldsymbol{K}$ AND $\boldsymbol{W}$ , Ξ = -10MV ..... 40
FIGURE 17 : VELOCITY PROFILES AT DIFFERENT $\boldsymbol{K}$ RATIOS. ..... 42
FIGURE 18: $K_{EO}$ VERSUS $\boldsymbol{K}$ FOR DIFFERENT $\boldsymbol{W}$, Ξ = -10 MV ..... 43
FIGURE 19 : $K_{EO}$ AND $K_P$ , $\boldsymbol{W = 1}$ , Ξ = -10MV ..... 43
FIGURE 20: ELECTROOSMOTIC PERMEABILITY IN DIFFERENT $\boldsymbol{K}$ AND $\boldsymbol{W}$, FOR THE NONLINEAR PB EQUATION UNDER CONSTANT POTENTIAL OF -10MV ..... 44
FIGURE 21 : ELECTROOSMOTIC PERMEABILITY PROFILES, LINEAR VS. NON-LINEAR MODEL, Ξ= -10MV ..... 45
FIGURE 22 : THE DISTRIBUTION PROFILE OF ELECTROOSMOTIC PERMEABILITY, NON-LINEAR PB WITH CONSTANT CHARGE, $\boldsymbol{\sigma = 0.2\ C.m-2}$ ..... 46
FIGURE 23 : ELECTROOSMOTIC PERMEABILITY IN DIFFERENT$\boldsymbol{K}$, $\boldsymbol{\sigma = 0.2\ C.m-2}$ ..... 46
FIGURE 24 : COMPARISON BETWEEN ELECTROOSMOTIC AND HYDRODYNAMIC PERMEABILITY IN NON-LINEAR PB MODEL USING CONSTANT CHARGE BOUNDARY CONDITION. $\boldsymbol{\sigma = 0.2\ C.m-2}$ ..... 47
FIGURE 25 : THE PROFILE OF KEO AS A FUNCTION OF PH, AND $\boldsymbol{K}$ RATIO FOR $\boldsymbol{W = 1}$ . $\boldsymbol{\sigma max = 0.7\ C.m-2}$ ..... 48
FIGURE 26 : KEO PROFILES FOR DIFFERENT $\boldsymbol{W}$ VALUES UNDER PH EFFECT, $\boldsymbol{K}$=0.58 ..... 49

# 1. Introduction

Electroosmosis is an electrokinetic phenomenon, in which the flow of an electrolyte is driven by an external electric field, applied between the inlet and outlet and acting on ions existing near the channel walls(Afonso, Pinho and Alves 2012).

As electric charges are present in liquids, having them in contact with a charged surface would result in having a potential gradient on the charged surface and in the liquid as well. A solid- liquid interface can acquire electric charge through two ways: 1- adsorbing ions in the liquid or 2- ionization of the molecules of the solid (Ajaev 2012).

Electroosmotic effects have major role in quality of fluid transport in porous medium. Having known these effects, the confrontation with the problems related to transport phenomenon in porous medium would become easier to deal with. The examples may include, soil contamination, oil recovery. In addition, recently the application of the method has been extended to biological- chemical- medical analysis and new techniques in energy and geophysical engineering, especially in micro and nano scales (Wang and Chen, Electroosmosis in homogeneously charged micro- and nanoscale random porous media 2007). Also in the industrial field, electroosmosis is being implemented at mineral separation, assessment of battery performance, treatment of radioactive wastes, etc (Bowen and Clark 1983).

In recent years, electroosmosis has been used in order to remove pollution from the soil. The most important advantages of this method may be considered as following:

- This method can be performed as an in-situ application
- This method is particularly effective for the soils with low permeability and tight structures

Electroosmosis has been very effective in removing hydrophobic organic compounds (HOC), which has low volatility, low mobility, low solubility, and low degradability(Kim, et al. 2010). By applying an electric potential to a saturated porous medium, excess neutral cations

would move towards the cathode, dragging water along. At the same time, anions move toward the anode at a much lower rate, hence, the applied electric potential creates a net flow of water to the cathode, carrying the pollutions with it(Corapcioglu 1991).

## 1.1. Fundamentals of electrokinetics

To describe the electroosmosis notion, a channel with charged surfaces is being considered, which carries a Newtonian fluid, known as electrolyte. The motion of the electrolyte fluid is induced due to an electric field and is referred to as electroosmosis or electroendosmosis (Ajdari 1995). Usually, having a chamber containing a fluid under the influence of an electric field, the electrophoretic flow also exists. This flow is referred to the movement of particles in the fluid toward their opposite pole. The force acting on the moving particles is called "Electrophoretic Force" (Israelachvili 2011).

Having negatively charged surfaces in a chamber (which usually is the case for clayey soils), the above mentioned actions cause the excess positive ions (cations) move towards the cathode. These counterions remain in an atmosphere adjacent to the walls of the chamber, which is called the "diffuse (or electric) double layer (EDL)" and the whole liquid column enveloped by these ions will be dragged along with them. This phenomenon is known as the electroosmotic flow (EOF) (Israelachvili 2011) . Most substances when are brought into contact with a polar medium, acquire a surface electric charge, which results in formation of the electric double layer, compromising the charged surface and a neutralizing excess of counterions in the adjacent solution (Bowen and Clark 1983). The electric potential at the internal surface of the double layer is referred to as "zeta potential" (Israelachvili 2011).

As the liquid away from the boundaries is assumed to be electrically neutral, therefore, the only space, in which the density of the electric charges is nonzero is the electric double layer. The zeta potential characterizes the electric field in the liquid near the solid. This potential in case of having a uniform charge density on the surface, is only a function of one Cartesian coordinate, normal to the wall (Ajaev 2012).

The electric filed, which is the driving force for electroosmosis, is usually considered to be an external imposed field. However, it can also be an internal field, which occurs due to presence of heterogeneity of the ions on the surfaces of the channel. This heterogeneity generates electric potential gradients (Ajdari 1995). Moreover, Herr, et al., (2000) argue that having a non-uniform surface charge distribution can induce a pressure gradient as well.

Electroosmosis is controlled by the combination of electrokinetic and hydrodynamic forces that leads to the motion of a liquid phase in a porous body (Joekar Niasar, Schotting and Leijnse 2013).

The charged surfaces of the porous body control the surface reactions, transport phenomena and the wettability of the porous media(Joekar Niasar, Schotting and Leijnse

2013). However, surfaces are not being charged uniformly, as we are always faced with heterogeneity in natural domains. Non-uniform surface charge (zeta potential) distribution can cause the pressure gradient to induce(Herr, et al. 2000).

Therefore, heterogeneity is considered as an important factor in quality of the above-mentioned characteristics and its effects are being studied.

Another important factor is the interaction between the ions on the surface and the counter/co ions in the fluid. This phenomenon is also included in the model.

Having a charged surface, there would also be equal but opposite charged “counter-ions” in contact with it. Surface of the boundary is called “Stern” or “Helmholtz” layer. Next layer is in fact the atmosphere adjacent to the stern layer, which is called “diffuse electric double-layer”(Israelachvili 2011). Helmholtz and diffuse electric double-layer are shown in Figure 1.

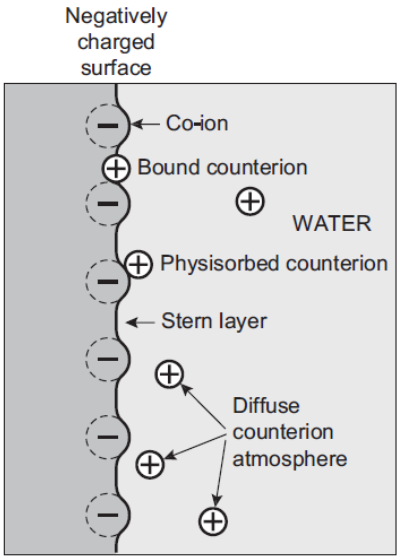


**Figure 1 : Helmholtz and diffuse electric double layer. (Israelachvili 2011)**

### 1.1.1. Debye length

The thickness of the diffuse electric double layer is defined as Debye length. It also describes the ionic atmosphere near the charged surface and it only depends on the properties of the solution, not the surface (Israelachvili 2011).

The electric potential distribution is of course related to the location of the Debye length. For 1:1 electrolytes (also called symmetric electrolytes e.g. NaCl), the counterions density is higher near the wall or within the Debye length, which leads to a higher potential at this area. By getting far from the Debye length, as the counterions concentration diminishes, the potential tends to zero as a result (Israelachvili 2011).

The thickness of Debye length ranges between several angstroms and 100 nm for typical ionic solutions used in applications. For pure water, it is of the order 1micrometer (Ajaev 2012).

The factors on which the thickness of the diffuse double layer relies are:

- Magnitude of the charge density on the soil surface
- The concentration of the ions in the pore fluid
- The valence of the cations
- The dielectric properties of the pore fluid

According to Acar, et al. (1995), when the electroosmotic permeability is at its maximum value the rate of electroosmotic mass flux is equal to the mass flux by migration.

Having a high ionic bulk concentration, the thickness of the diffuse double layer and the extent of the strain field resulting in the flow of pore fluid decreases and therefore, the electroosmotic pore fluid flux will be confined more to the margin of the channel.

In general, the Electroosmotic volumetric flow is at maximum level when the thickness of the diffuse double layer is at its highest level, and this happens when the ionic bulk (electrolyte) concentration is low or the water content is high (Acar, Galeb, et al. 1995).

However, this conclusion is true in Darcy scale, and not at pore scale. At pore scale, the electroosmotic permeability and electroosmotic velocity reach a peak and stay at a constant rate, which is given by Smoluchowski relation (Eq. 13). At small Debye length values, however, the velocity profile does not follow a fully developed profile. The electroosmotic permeability becomes lower by having overlapping EDLs.

Although large Debye lengths in comparison with the channel width can result in their overlapping, this causes the electric potential not being able to reach a zero value even at the middle of the channel. Overlapping of the electric double layers causes a reduction in electroosmotic velocity. It will also induce peak dispersion due to a transition in nature of the velocity profiles (Talapatra and Chakraborty 2007).

At Darcy scale, the flow cross section consists of a number of pores, at each of which the velocity reaches a fully developed profile. The fluid flow at this state becomes high due to having more perimeter of contact between solid and water. This fact takes place solely at the state, where we are faced with the fine-grained material. Having a large fluid-solid contact perimeter at this situation results in having higher flow, as the electroosmotic flow is higher at the surfaces.

The electroosmosis phenomenon is dependent on the nature of the double layer. High ionic strength of the solution (0.001 M) results in small Debye length and a thin double layer in comparison with the channel width. At this situation, the electroosmosis velocity becomes directly proportional to the zeta potential (Kim, et al. 1996).

## 1.2. Literature review and previous studies

Since 200 years ago, numerous experimental and theoretical investigations have been performed on electroosmotic flows (EOF) in porous media, due to their vast applications in soil, petroleum, and chemical engineering. (Wang, Pan, et al. 2007)

The first electrokinetic effects were observed by Reuss in 1809 in an experimental investigation on porous clay. Since then, remarkable number of studies has been undertaken in electroosmosis; new techniques have been suggested and found in energy and geophysical engineering (Wang, Pan, et al. 2007). In these studies, different important factors, which affect electroosmotic phenomena, have been investigated. Here a short description of the application is provided.

### 1.2.1. Electroosmosis in soil remediation

The studies of Acar et. al have been one of the important ones on the principles of electroosmosis. In their study, they have represented an overview of the principles of the electrokinetic remediation techniques in soil remediation. They argued about the types of pollutants and media in which the technology can be used (Acar, Galeb, et al. 1995).

They have also performed another experiment on principles of the electrokinetic remediation, focused on electrokinetic permeability and the governing factors of it, including pH change. According to the authors, Migration of the ions $H^+$ and $OH^-$ is one factor, controlling the pH across the mass. The ionic mobility of Hydrogen ion is about 1.8 times the mobility of the Hydroxyl ion. This fact should be taken into account when studying the behavior of the electrokinetic phenomena. These experiments have indicated the necessity of the control over the chemistry of the field. Zeta potential has been reported to decrease linearly with the logarithm of the pH of the soil medium. The authors have also argued that although the fluid flow due to the hydraulic gradient is highly affected by the soil's macrostructure, the electroosmotic flow is merely dependent on the porosity and surface chemistry, and not the pore size distribution or presence of macro pores. That is why the electroosmotic flow is an effective method for generating a uniform fluid and mass flow in fine-grained soils (Acar and Alshawabkeh, Principles of Electrokinetic remediation 1993). Figure 2 is a schematic diagram of the ionic species near the surface of clay and the velocity profile of electrolyte, generated by Acar, et al.(1995).

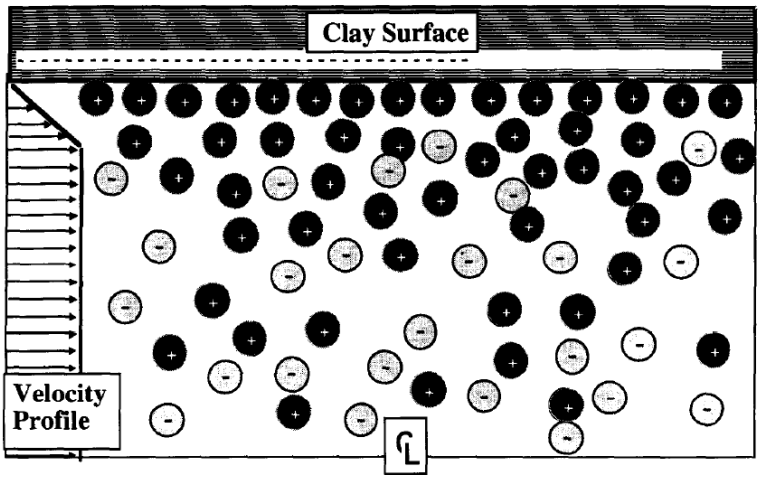


**Figure 2 : A schematic diagram of the alignment of ionic species within the electric field developed by the soil surface and the pore fluid velocity profile generated when an electric field is applied along the capillary normal to the direction of the electric field of the surface. (Acar, Galeb, et al. 1995)**

### 1.2.2. Important factors in electroosmosis

Here, we focus on two major factors influencing electroosmosis: pH and pore geometry.

#### pH

In a study by Leland and Gwen (1997), the relation between the zeta potential and electroosmotic permeability is being discussed and the effect of electrolyte properties (such as PH, ionic strength, divalent metal ion concentration) on clay particle zeta potential is being studied. The investigations are being carried on for two different clayey materials, namely, Georgia kaolinite and Wyoming bentonite. The difference between the results for the two mentioned materials is being discussed as well. All the factors are considered to have effect on zeta potential, which itself has a direct relation with the electroosmotic permeability and its changes.

Necessity of pH control in electroosmotic pumping has been studied by Nerine, et. al (2003). In their experiment, they indicate the importance of PH control between anode and cathode reservoirs. Their first experiment without PH control, metal and carbonate precipitation occurred near the cathode end of the domain, while near anode acidification took place. The result of this acid and base precipitation near the cathode and anode ends of the core was reduction in electroosmotic flow in the pore volume.

Another study about the effects of the pH on electroosmosis was performed by (Lemaire, Moyne and Stemmelen 2007). In their model, they specify the dependence of the surface charge density of clay on pH effects and ionic strength (Lemaire, Moyne and Stemmelen 2007).

The authors have used two types of modeling, one with considering the PH effects and the other without considering it, but both are trying to highlight the necessity of considering the surface reactions in studying electroosmosis.

According to their model, by not considering the PH effects in the model, the results of virtual bulk pressure distribution profile does not agree with the experimental results of soil remediation workers , Eykholt(1997) and Alshawabkeh and Acar (1996). In the experiments, a negative pressure of a few kilopaskals was observed while the model represented only positive pressures. According to other experimental data, (Casagrande, 1952; Esrig, 1968) negative pore pressure is often being observed in electroosmotic dewatering and consolidation of soft soils. In brief, the results of the (Lemaire et al.) model show the necessity of considering the effect of electrochemical couplings on hydraulic properties.

In the second model, the effects of PH and ionic force are considered to create a non-uniform surface charge density, resulting in a non-uniform electroosmotic process, as a result, the negative pressure (suction) of a few thousands of Pascal can be observed in the model.

The authors showed that their approach in explanation of electroosmosis migration is highly sensitive to factors such as structural surface charge density, geometric effects, Debye length and temperature. As an example, they argued that the significance of the electroosmosis process declines when the ratio between the inter platelet distance and the Debye length increases.

### Geometrical and Physical factors

Another important issue is the geometrical factors that influence flow and transport. For example, Kang, et. al,(2004) have studied the effect of geometrical and electrokinetic parameters on a series of parallel tortuous tubules. In their study, a model is being developed to explain the electroosmotic flow in a charged microcapillary. The microcapillary was being packed tightly with charged microspheres. The schematic view of this microcapillary series is being shown in Figure 3.

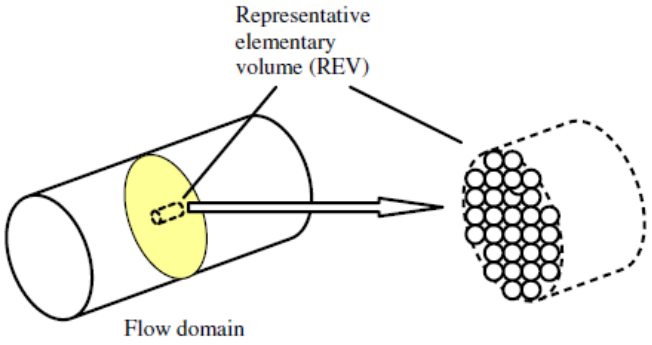


**Figure 3: Schematic illustration of representative elementary volume (REV): the length scale of the REV is much larger than the pore scale, but considerably small (Kang, Yang and Huang 2004)**

They have studied how the electroosmotic flow (EOF) in the understudy microcapillary was being affected by the geometrical and electrokinetic parameters. The model is being solved under three different conditions, full numeric solution, analytic solution, and slip velocity approximation theory, and then a comparison between the three methods is being made. However, they have investigated the channel in a constant potential boundary on the walls, and the chemical effects are not taken into account. The behavior of a charged particle in the channel is being studied in terms of its Darcy velocity in different conditions of potentials on its surface and the ratio between the surface charge of the particle and the walls of the channel.

In general, they introduce a series of factors which have effect on the EOF in microcapillary tube, to name a few, the properties of the fluid, porosity and tortuosity, the size of the capillary and its ratio to EDL, the charge condition of the surfaces adjacent to the fluid. The important result is that in case where the size of the capillary is comparable to the size of the charged particle (which can be assumed a situation like having two charged surfaces, as they are comparable in size) the electrokinetic wall effects become stronger. Furthermore, having a highly negative charge on the capillary walls, results in enhanced EDL. Otherwise, by having a small magnitude of charge on the walls, the EDL becomes weak and in that case, even the flow direction can be reversed (Kang, Yang and Huang 2004).

Wang and Chen (2007) investigate the major geometrical factors in EOFs through their numerical model.

They use a mesoscopic simulation method, which performs a random generation growth method for three-dimensional random microstructures of porous media. For solving the non-linear equations of electroosmosis for 3-D porous media, they use a lattice Boltzmann algorithm.

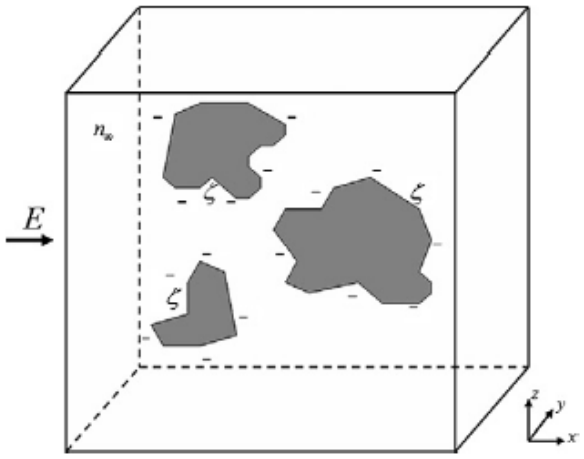


**Figure 4: Schematic illustration of EOF in charged random porous media.(Wang and Chen, Electroosmosis in homogeneously charged micro- and nanoscale random porous media 2007)**

Wang, et al.,(2007), showed that the electroosmotic permeability increases monotonically with the porosity of the porous media(Figure 5). The increasing rate also grows with the porosity of the media.

The electroosmotic permeability also increases with the grain size and bulk ionic concentration in a given porosity. The linear relationship between the electroosmotic permeability and zeta potential on solid surfaces is only limited to high zeta potentials.

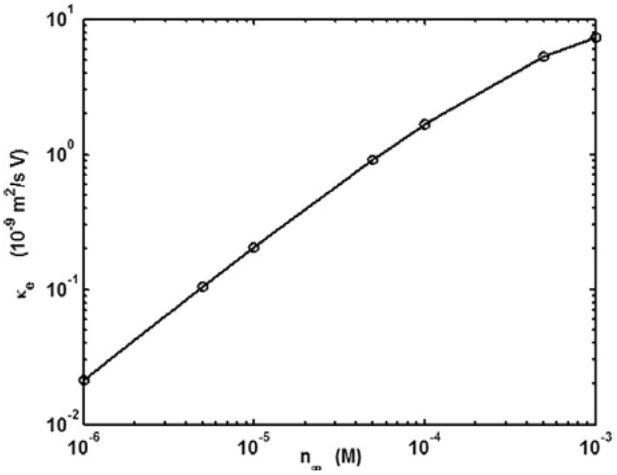


**Figure 5 : The electroosmotic permeability changing with the bulk ionic concentration. ε = 0.38, ζ =–50 mV, and E = 1 ×10$^4$ V/m.(Wang and Chen, Electroosmosis in homogeneously charged micro- and nanoscale random porous media 2007)**

They argue that these results are also being confirmed through the current available experiments. They claim, but not true, most of the previous theoretical models have two

major defects in predicting the EOF's in micro and nano channels. First, is that most of them are based on thin electric double layers(EDL's), which results in not being able to have channels with the same thickness of the EDL. Second, these theoretical models are weak in providing the flow structure details; therefore, a deep understanding of the transport mechanism of the electroosmosis cannot be obtained (Wang and Chen, Electroosmosis in homogeneously charged micro- and nanoscale random porous media 2007).

## Objectives

The aim of this study is to determine the electroosmotic permeability in a rectangular channel to different factors. These factors include heterogeneity of the charged surface in terms of zeta potential, the dimensions of the channel compared to the Debye length, the chemical effects such as pH magnitude. According to these mentioned facts, geometrical variables include the dimensionless length ratios of the dimensions of the rectangular channel, which is being named as $\overline{W}$ ratio, and the ratio between the smaller dimension of the channel compared to Debye length, which is referred to as $\overline{K}$ ratio. Therefore, the electroosmotic permeability is being introduced as a function of these dimensional factors and pH effects.

In order to obtain the electroosmotic permeability as a function of mentioned factors, Poisson-Boltzmann equation has been solved. The results have been obtained by solving linear and non-linear equation and the results of the two methods have been compared. The detailed explanation of the equation and the linearization of it has been mentioned at section 2 of the current study.

As another important effect on the magnitude of electroosmotic permeability, two types of boundary conditions have been studied and the results of both types of boundary conditions (constant potential and constant charge) on particle surfaces have been compared. The compatibility of the results with the previous theoretical and experimental investigations has also been discussed.

Some of the mentioned factors can have significant effects on the ion regulation on the surfaces and in the solution, which can also result in the different behaviors of the system in terms of fluid flow between the charged surfaces and the ions' movement as well as the electroosmotic permeability. The effects of these factors in determining the magnitude and profiles of the electroosmotic permeability and each parameter's role, compared to the other factors is the main question of this study.

# 2. Governing Equations

## 2.1. Poisson- Boltzmann equation

In the introduced channel system with the electrolyte fluid, the present active ions of the system are the dissociated ones from the surface and the electrolyte ions (i.e. the ions of the electrolyte that have been dissociated due to the contact between fluid and solid surface). The interaction between these ions results in occurrence of electro osmotic forces, as well as coulomb forces, which depend on several factors. These factors are electrostatic potential (Ψ), concentration of ions ($C$), and valence of the ions ($Z_i$ ). The Poisson equation reads as:

$$\nabla^2 \Psi = -\frac{\rho_e}{\varepsilon} \quad \text{Eq. 1}$$

Where Ψ denotes the potential in Volts, $\rho_e$ the charge density in Coulombs per square meter, and $\varepsilon$ the permittivity of the medium in Farad per meter.

The Boltzmann distribution equation can be used in order to express the charge density distribution. The Boltzmann equation is as follows:

$$C = C_b \exp\left(-\frac{Z_i\, e\ \Psi}{k_B\, T}\right) \quad \text{Eq. 2}$$

With $C$ as concentration of ionic species in electrolyte with the unit of mol per liter or mol per cubic meter(mM), $C_b$ is the bulk concentration of the ions or the concentration of the ions where, $\Psi = 0$. $Z_i$ is the valence of the ion. $e$ denotes the charge of an electron with positive sign in coulombs. $k_B$ denotes the Boltzmann constant in Joules per Kelvin, and T denotes temperature in Kelvin.

According to Boltzmann distribution, having negatively charged ions on the surface, the surface number density of ions can be expressed as follows:

$$\rho_e = -2\, C_b\, Z_i\, e\ \sinh\left(-\frac{Z_i\, e\ \Psi}{k_B\, T}\right) \quad \text{Eq. 3}$$

Having the above-mentioned equations, the Poisson-Boltzmann equation reads as:

$$\nabla^2\, \Psi = 2\,\left(\frac{C_b\, Z_i\ N_A\, e}{\varepsilon}\right)\ Sinh\left(\frac{e\, Z_i\ \Psi}{k_B\, T}\right) \quad \text{Eq. 4}$$

With $N_A$ as the Avogadro number. ($mol^{-1}$)

The equation is being simplified for a special case of having two types of ions, or a symmetric electrolyte.

In order to solve the Eq. 1 analytically, the equation is at first being linearized. In order to do so, $Sinh\left(\frac{e\, Z_i\ \Psi}{k_B\, T}\right)$ should be replaced by$\left(\frac{e\, Z_i\ \Psi}{k_B\, T}\right)$. This linearization can is only valid for $\left(\frac{e\, Z_i\ \Psi}{k_B\, T}\right) \ll 1$.

Although Eq. 4 has been criticized by Onsager(1933) and Kirkwood(1934), as being only valid for small amounts of $Z_i\, e\ \Psi$ compared to $k_B\, T$ , however, Casimir(1944) has pointed out that the criticism is valid for double-layers around separate ions, but the equation can be used for larger surfaces containing many elementary charges (C. Prievet and Ruckenstein 1976).

In fact, Eq. 4 is the result of applying the relationship between ion distributions Eq. 3 and the electrostatic potential profile. It is assumed that the electrolyte between the charged surfaces consists of ions of valence equal to unity and the electrolyte is symmetric, therefore, as an example of an electrolyte with mentioned characteristics, NaCl can be considered.

Eq. 3 implies that the electric charge density in nonzero in the double layer, which means that by applying an electric field onto this part the movement of the fluid can be induced or controlled. This fact is the origin of the Electroosmotic flow. (Ajaev 2012)

## 2.2. Debye length

Debye length is denoted by "$\lambda_D$" and is defined as the characteristic length scale over which significant charge separation can occur(Joekar Niasar, Schotting and Leijnse 2013). It is also being denoted by $\frac{1}{\kappa}$ in the literature.

Deby length is inversely proportional to the square root of ionic strength,"$\frac{\Gamma}{2}$".

$$\lambda_D = \sqrt{\frac{\varepsilon\, k_B\, T}{2\, e^2\, (\frac{\Gamma}{2})}} \quad \text{Eq. 5}$$

$$\frac{\Gamma}{2} = 0.5\, \sum_i C_{b_i}\, N_A\, Z_i^2 \quad \text{Eq. 6}$$

It is apparent from the equations that having a larger ionic strength results in smaller Debye length. This can also be regarded as the fact that larger ionic strength means having more ionic interaction and therefore, having the ionic atmosphere (diffuse double layer) closer to the surface.

## 2.3. The Electroosmotic Flow

As mentioned before, in order to have the electroosmosis effects in the system, there must be an applied electric field ($E_x$) on it, which forces the ions to move, dragging the fluid with them. Obviously, by applying such condition, the fluid will contain a characteristic velocity, which is under investigation at this step. First, the equation of motion of a liquid in laminar conditions with constant density and viscosity is introduced as follows:

$$\rho \frac{\partial u}{\partial t} + \rho u \,.\nabla u = -\nabla p + \mu \nabla^2 u + F \quad \text{Eq. 7}$$

As we are assuming that the flow is steady, two dimensional and fully developed$\frac{\partial u}{\partial x} = 0$ , the velocity components are nonzero only in the direction parallel to the channel's length. Therefore, the other components of the velocity would be equal to zero. This yields:

$$\boldsymbol{u = u_x\,(y, z)} \quad \textbf{Eq. 8}$$

$$v = 0$$

$$w = 0$$

Where, "u" is the x component of the velocity and "v" and "w" are its components in y and z direction respectively Eq. 8 also declares that the velocity profile only exists in y and z direction, as the flow is steady in x direction. Another assumption made is that there is no external pressure gradient, therefore the first term in right hand side of Eq. 7 becomes zero

and the only force acting on the fluid would be the electric field applied on the system. (Arulanandam and Li 2000)

As a result, the general form of Eq. 7 becomes a balance between the viscous stresses in the fluid and the external electric field, which is proportional to the imbalance between the ions or net charge density.

$$\mu\left(\frac{\partial^2 u}{\partial y^2}+\frac{\partial^2 u}{\partial z^2}\right)=F_x \quad \text{Eq. 9}$$

$$F_x=\rho_e E_x \quad \text{Eq. 10}$$

Substituting Eq. 10in Eq. 9, and replacing $\rho_e$ from Eq. 3, results in :

$$\mu\left(\frac{\partial^2 u}{\partial y^2}+\frac{\partial^2 u}{\partial z^2}\right)=\left(\frac{2\,C_b\,Z_i\,e}{\varepsilon}\,\sinh\Psi\right)E_x \quad \text{Eq. 11}$$

Electroosmotic permeability, $K_{eo}$ ($m^2V^{-1}s^{-1}$ ) is given by Eq. 12. (Wang and Chen, Electroosmosis in homogeneously charged micro- and nanoscale random porous media 2007)

In order to explain the notion of electroosmotic permeability, the Helmholtz-Smoluchowski theory for Electroosmosis should be considered. The pore fluid transport under an electrical potential difference is widely being described by the Helmholtz-Smoluchowski theory for electroosmosis. The theory also introduces the electroosmotic permeability, Keo as the volume rate of water flowing through a unit cross-sectional area due to a unit electrical potential difference (cm2/V.s). Keo is a function of the effective bulk electrical conductivity of the soil. (Siemens per centimeter) (Acar and Alshawabkeh, Principles of Electrokinetic remediation 1993)

$$K_{eo}=\frac{u}{E_x} \quad \text{Eq. 12}$$

Therefore, the $K_{eo}$ can be represented as a function of $\overline{K}$ and $\overline{W}$.

The highest value for electroosmotic permeability can be calculated at this boundary condition, using the Smoluchowski equation. This equation represents a value for electroosmotic velocity as a function of zeta potential, electric field, permittivity of the medium and viscosity and it is fully independent from the pore geometry.

$$K_{eo}=\frac{u}{E_x}=\frac{\varepsilon\,\xi}{\mu} \quad \text{Eq. 13}$$

## 2.4. The Hydrodynamic Flow

In case of having a hydrodynamic pressure instead of the electroosmotic pressure, then the velocity of the flow, will solely depend on this hydrodynamic pressure. The velocity in its general form can be decoupled with three components, which can be mentioned as

hydrodynamic, electroosmotic, and osmotic.(Joekar Niasar, Schotting and Leijnse 2013) Here, it is being assumed that the last two components do not exist and the only present velocity is being created by the hydrodynamic pressure gradient. According to (Joekar Niasar, Schotting and Leijnse 2013), this velocity can be represented through the following equation.

$$u_p = -\frac{32\,h^2}{\mu\,\pi^5 \bar{W}} \sum_{n=1}^{m} \left(\frac{1}{(2n-1)^5}\left((2n-1)\pi\,\bar{W} - 2\tanh\left(\frac{(2n-1)\pi\,\bar{W}}{2}\right)\right)\right) \partial_x P_b \quad \text{Eq. 14}$$

Where h is the half height of the channel, μ, is the fluid viscosity, and $P_b$, is the bulk fluid pressure. Here, m is the total number of the pores in the system.

In equation- 20, by omitting the pressure gradient term and the fluid viscosity at the right hand side, the remaining statement will be representing the Hydraulic pressure permeability, which has the unit of $m^2$. This can be regarded as the Hydraulic equivalent of the $K_{eo}$, and is denoted by $K_p$.

By dismissing the osmotic component of the velocity, the total velocity in the rectangular channel can be represented as:

$$u = K_p \nabla P + K_{eo} E_x \quad \text{Eq. 15}$$

## 2.5. Inclusion of pH effects on surface charge

As mentioned before the effects of pH on electroosmosis are among the most important factors. The effects of considering and not considering pH in the EOFs have been widely studied by previous authors.

In the current study, the pH sensitivity test has been carried out for two surface charge conditions of 0.7 and 0.07 $Cm^{-2}$. The mentioned surface charge of course, is the maximum charge of the surface, which is being explained as the maximum exchanged charged density, in other words, the case when all the surface sites have reacted. (Lemaire, Moyne and Stemmelen 2007) According to the authors, the reactive sites of the clay surface are the hexagonal cavities, which can adsorb a proton or a monovalent cation (e.g. sodium ion). The total surface density of the reactive sites ($N_x^{tot}$) is as follows:

$$N_x^{tot} = 7.2457 * 10^{-6}\ \frac{mol}{m^2} \quad \text{Eq. 16}$$

Having the electrolyte consisting of NaCl, the reactions of the ions and the water compartments with the surface sites are as follows:

The proton exchange:

$$X + H^+ \leftrightharpoons XH^+$$

And sodium exchange:

$$X + Na^+ \leftrightharpoons XNa^+$$

Maximum charge density is defined as :

$$\sigma_{max} = F\, N_x^{tot} = 0.699\ C/m2$$

Where, F is the Faraday's constant.

Then the net proton charge density and complexation charge density are:

$$\sigma_H = \sigma_{max}\, x_{XH}$$

$$\sigma_C = \sigma_{max}\, x_{XNa}$$

As

$$\sigma_f = \sigma_0 + \sigma_{max}\,(x_{XH} + x_{XNa})$$

Then

$$\sigma_f = \sigma_0 + \sigma_{max}\,\frac{K_{Na}[Na] + K_H[H]}{1 + K_{Na}[Na] + K_H[H]} \quad \text{Eq. 17}$$

Where $K_{Na}$ and $K_H$ are the equilibrium constants for the chemical reactions of Na and proton. $X_i$ is the mole fraction of considered species. (Lemaire, Moyne and Stemmelen 2007)

The surface charge density$\sigma_f$ is being used in order to obtain the boundary condition on the surfaces of the channel. According to the following equation, the potential gradient on the channel wall, which is the boundary condition of the domain, is related to the surface charge.

$$\nabla\Psi \,.\, n = \frac{\sigma_f}{\varepsilon} \quad \text{Eq. 18}$$

In Eq. 18, electric potential is denoted byΨ, surface charge by$\sigma_f$, and n is the unit vector normal to the surface.

## 2.6. Numerical solution

### 2.6.1. Linear PB equation

To model P.B equation, it must be first discretized. For a second derivative function, the general discretized form in one dimension is:

$$\nabla^2\Psi = \frac{\Psi_{i+1} - 2\Psi + \Psi_{i-1}}{\Delta x^2} \quad \text{Eq. 19}$$

As the domain is in Cartesian system, it has two coordinates and so two independent variables (x and y) and the unit vectors for them are (i and j) respectively. This is the situation for the 2- dimensional model. Of course for the 3-D model the number of independent variables as well as the unit vectors would be three. The following equations will also have an additional term for the third dimension. Here, for simplicity only the 2-D discretization equations are mentioned as there would not be a large difference between these equations and the 3-D equations. Therefore, Eq. 19 becomes:

$$\nabla^2\Psi = \frac{\Psi_{i+1,j} - 2\Psi_{i,j} + \Psi_{i-1,j}}{\Delta x^2} + \frac{\Psi_{i,j+1} - 2\Psi_{i,j} + \Psi_{i,j-1}}{\Delta y^2} \quad \text{Eq. 20}$$

From Eq. 4 it is known that the right hand side of the last equation is equal to:

$$\alpha = 2\left(\frac{C_b\, N_A\, e}{\varepsilon}\right)\left(\frac{e\, Z_i\, \Psi}{k_B\, T}\right)$$

For simplicity, all the parameters of the above statement can be assumed as a coefficient for $\Psi$ equal to a constant, α. On the other hand, as the grid sizes of the domain are assumed equal, so:

$$\Delta x = \Delta y = \Delta h$$

Therefore, Eq. 20 becomes:

$$\nabla^2\Psi = \frac{\Psi_{i+1,j} - 2\Psi_{i,j} + \Psi_{i-1,j} + \Psi_{i,j+1} - 2\Psi_{i,j} + \Psi_{i,j-1}}{\Delta h^2} = \alpha\Psi_{i,j}$$

$$\nabla^2\Psi = \Psi_{i+1,j} - 2\Psi_{i,j} + \Psi_{i-1,j} + \Psi_{i,j+1} - 2\Psi_{i,j} + \Psi_{i,j-1} = \alpha\,\Delta h^2\,\Psi_{i,j}$$

$$\Psi_{i+1,j} + \Psi_{i,j+1} + \Psi_{i-1,j} + \Psi_{i,j-1} - (\alpha\,\Delta h^2 + 4)\Psi_{i,j} = 0 \quad \text{Eq. 21}$$

Having the equation discretized, it can be solved through the following matrix equation:

$$A\,\Psi = B \quad \text{Eq. 22}$$

Where, “A” is a matrix consisting of coefficients of "$\Psi$" in Eq. 4. In the model, it determines if each node has another node in its vicinity or it has reached the boundary of the domain. “B” is called the right hand side matrix. It consists of the constant values in the same equation and is responsible for the boundaries of the whole domain and the magnitude of

the zeta potential at these parts. These magnitudes will be added to the model as a coefficient for each boundary. They determine if the model is “homogeneous” or “heterogeneous”. Having equal values for entries of the “B” matrix means that the magnitude of the zeta potential is constant among the walls of the channel, therefore, the model is homogeneous. In contrary, a heterogeneous model consists of different values of entries along the domain, which can be fully randomly chosen or containing a specific order. "$\Psi$" is the unknown matrix in the equation and must be solved numerically. The sizes of the matrices are determined according to the size of the domain and the grid size.

### 2.6.2. Boundary and Initial Conditions

The boundaries of the domain are determined by introducing the matrix “B.” As mentioned before this matrix shows at which cell the domain meets the boundary. For each cell, presence of another cell in the vicinity means the corresponding entry on the matrix is equal to one. Otherwise, the entry would be zero. The domain is a rectangular, which has charged surfaces at boundaries. The magnitude of electric potential of the surfaces (zeta potential) is set in matrix “B.” At first, it is assumed that the charge of each surface is equal to one(negative charge). By this way, it is scaled to the reference potential. At further steps, the boundary condition changes from constant potential to constant charge on the surfaces of the channel. The latter situation is supposed to be more realistic, as it can determine the different values for the zeta potential, and as it is not possible to determine the zeta potential values independently.

### 2.6.3. Homogeneous and Heterogeneous Surfaces

In natural media, the solid surface is usually charged heterogeneously. Surfaces with different charges will have different electric potentials and affinity to the ions, which cause the interactions between the ions to behave since the maximum or minimum interaction energy usually, occurs below the Debye length (Israelachvili 2011), the heterogeneity effect would be considerable at overlapping EDL conditions.

In a natural porous media, there is heterogeneity at micro-scale. However, at the pore scale, many simulations with homogeneous boundary conditions have been done. At the current study’s simulations, heterogeneous zeta potential have been applied to show its effects on the electric field.

### 2.6.4. Non-linear PB equation

Non-linear PB equation has been solved for three different conditions, two of which contain the different boundary conditions of constant potential and constant charge on the surface, and another condition has been the constant charge boundary condition with consideration of the pH effects on the surface potential gradient.

In constant potential boundary condition, the procedure has not been much different from the linear procedure, as a value for the zeta potential as the boundary condition was determined and the complete PB non-linear equation was solved.

For solving the non-linear constant charge boundary condition, as the value of the zeta potential was unknown, the gradient of the electric potential over the surface was applied in composing matrix B, given Eq. 18. Having the gradient value for each two adjacent nodes, the electric field and consequently the stokes equation (Eq. 11) was solved.

The same procedure was carried on in order to calculate the electroosmotic velocity, when the pH effects were taken into account. The difference between the two procedures, however, was the fact that in the latter case the value for the surface charge density was calculated numerically, regarding the chemical state of the electrolyte. Having the value of the $\sigma_{max}$ (the maximum charge density), the value of surface charge density was calculated through Eq. 17. After solving the electric field, the values for ions next to the solid boundary was calculated. Having the local density of ions made it possible to recalculate the charge density using Eq. 17 again. The new charge density will change the boundary condition for the nonlinear PB equation. This cycle was repeated till a convergence is obtained.

Having the non-linear PB equation solved in terms of velocity, the electroosmotic permeability was calculated through Eq. 12.

## 3. Numerical Examples for Electric Field

The model has been developed in FORTRAN language. The visualization of the results has been made in Paraview® and MATLAB. For the two-dimensional model, width and height of the domain are inputs of the code, being divided by the grid size; yield the number of nodes in horizontal direction, and vertical direction. For 3-D model, another dimension represents the length or depth of the channel. The calculations, though, would not be different and all the mentioned steps can be followed for the 3-D model.

The two different models and their details are being explained as follows. First, the 2-D model is represented, followed by the 3-D model review. Having both models introduced in terms of the geometry, values and examples, the result and discussion parts of potential distribution, fluid velocity, and flow for each of them are being studied.

The initial 2-dimensional model consists of two parallel charged surfaces. It is assumed that the domain consists of a 2-D channel with the entry of the fluid on one side and the exit at the other side. The top and bottom as can be seen in Figure 8 are the charged surfaces with constant potential. The length of the parallel surfaces are equal to 4 micro meters and there is a 2 micrometer gap between them, which is assumed to be filled with a non-compressible fluid (e.g. water). The surfaces are charged with the homogeneous potential of -1 microvolts. Figure 8 and Figure 9 show the initial 2-D model, charged homogeneously with the mentioned dimensions. $C_b$ concentration is different in the two figures. As mentioned before, at higher $C_b$'s as the Debye length becomes small, the effect of double layer overlap is not seen. (Figure 8)

As shown in Figure 9, having a very small $C_b$, the double layer overlapping occurs and it can be seen that the value of electric potential does not reach zero at the mid-plane of the channel. It should be mentioned that both of these calculations are representing an equilibrium condition of the system, where there is no motion and all the ions are in static situation.

To check the accuracy of the numerical code, the results are compared with the analytical solution for a specific geometry.

## 3.1. Two-dimensional Example

Considering the 2-D model shown in Figure 6 and Figure 7, a comparison is being made between the two $C_b$ concentrations at a 1-D plane of the domain (from the surface to the mid plane). Again, a cross section is being considered and the electric potential from the channel wall to the mid-plane of it is under study. Figure 6, shows the distribution of the electric potential at $C_b = 0.0005\ mM$ and $C_b = 0.05 mM$. Of course, the channel is being rotated by 90 degrees; therefore, the wall of the channel is seen vertically. In order to have a reference to know how accurate the model is, at this step, the numeric model is being compared with the analytical solution.

## 3.2. Model verification

Solution to the Poisson-Boltzmann equation is being carried on through the linear equation, since this is the usual method in solving such non-linear equations due to its simplicity. The simplified Poisson-Boltzmann equation is derived by replacing the hyperbolic part of that by a first order Taylor series expansion. The simplified form of the equation in one dimension is as follows:

$$\frac{\partial^2 \Psi}{\partial y^2} = C_b Z_i^2 \Psi \quad \text{Eq. 23}$$

For a semi-infinite domain, in which the double layer is thin in comparison with the width of the channel, the bulk fluid can be treated as being at infinity. At this situation, the result is in

an exponential solution. While the origin is at the wall and the boundary conditions are $\Psi = 0$ at $y = \infty$ and $\Psi = \Psi_0$ at $y = 0$ (Kirby 2010).

The result is :

$$\Psi = \Psi_0 \exp\left(\frac{-y}{\lambda_D}\right) \quad \text{Eq. 24}$$

If double layers are not thin, the effects of the other walls must be taken into consideration. For two parallel plates (Figure 8), by a distance of 2d and origin $y = 0$ set at the midpoint, the boundary conditions can be satisfied with the hyperbolic cosine solutions of the linearized Poisson-Boltzmann equation. With $\Psi = \Psi_0$ at $y = -d$ and $y = d$ (Kirby 2010) , as follows:

$$\Psi = \Psi_0 \frac{\cosh\left(\frac{y}{\lambda_D}\right)}{\cosh\left(\frac{d}{\lambda_D}\right)} \quad \text{Eq. 25}$$

Using Eq. 25, the analytical solution to the model is being calculated and the model is being run for this condition. The numerical and analytical models for a 1-D cross section are compared to show the electric potential distribution profiles from surface to the mid plane of the channel. In Figure 7, the difference between the results of numerical and analytical solutions can be seen in different colors. As it is indicated in the figure, they have relatively low difference and it can be concluded that the numeric model can be used with a reasonably low error.

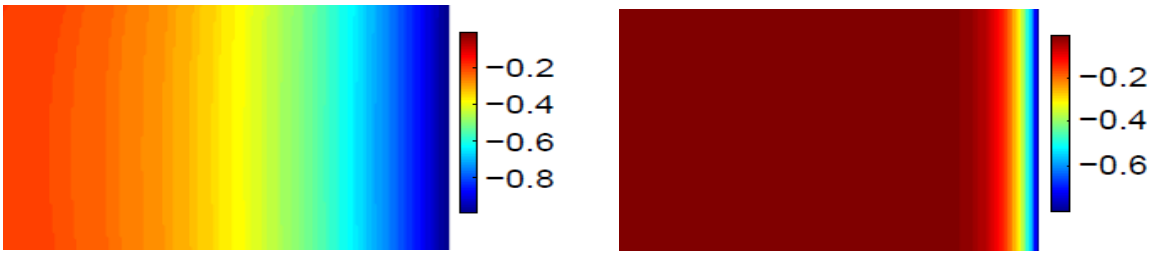


(a) (b)

**Figure 6 : Electric potential distribution when $C_b$ is equal to (a) 0.0005 mol/m$^3$ and (b) 0.05 mol/m$^3$**

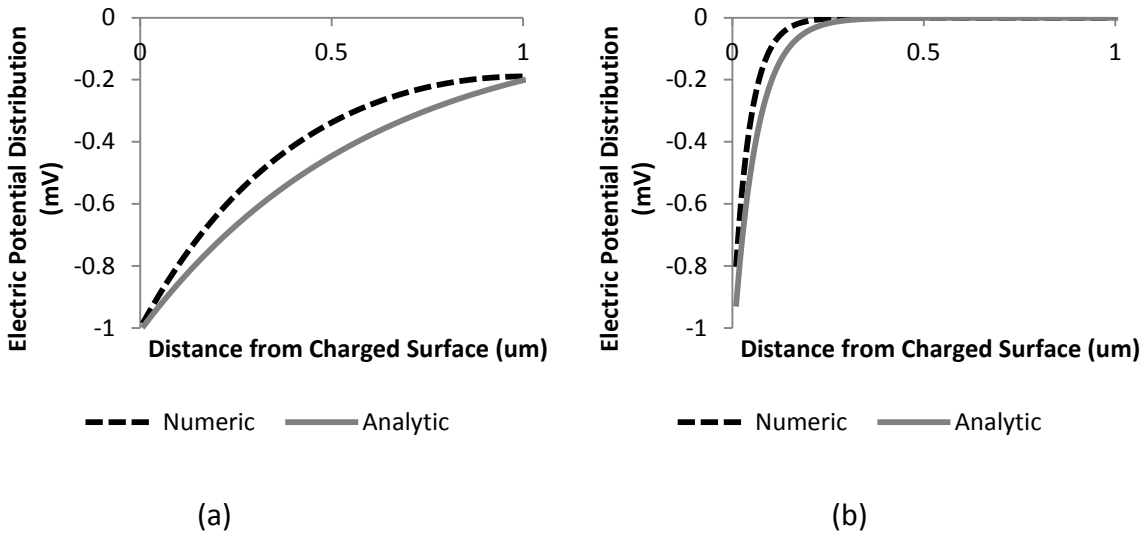


**Figure 7 : Difference between linear PB numerical and analytical solutions when $C_b$ is equal to (a) 0.0005 mol/m$^3$ and (b) 0.05 mol/m$^3$**

In Figure 6, the distribution profile of electric potential is being shown. In Figure 6(a) the $C_b$ concentration is equal to 0.0005 mol/m$^3$, which according to Eq. 5 makes the deby length to become greater in magnitude and as we know, larger deby lengths between the two parallel surfaces cause the overlapping of the double layers of the surfaces to happen, which is the situation in Figure 6(a) and the electric potential does not become equal to zero even at the mid plane. This phenomenon is also being observed in Figure 7(a) where neither numeric nor analytic solutions reach the zero potential, indicating that there is still potential profiles present at the mid plane of the channel.

In Figure 6(b), by having a larger $C_b$ , deby length decreases dramatically. Therefore, there would be no double layer overlap and the potential profile reaches zero almost near the surface in about 0.25 micrometers away from it. Figure 7(b) also indicates this fact by showing that the potential profile reaches zero way before the mid-section of the domain.

At this step, a 1-D section of the model is being used in order to examine the above-mentioned characteristics. By using a full 2-D section of the domain, the calculations would have had an additional dimension, which made them more complicated while the same results could be seen. Therefore, the examination of the model at this step is being done through the 1-D plane of the domain.


**Figure 8: Two homogeneously charged surfaces containing a Newtonian fluid. $C_b$ =0.05 mol/m$^3$**

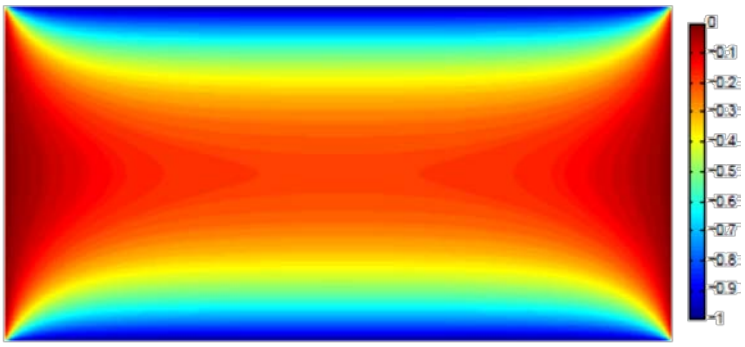


**Figure 9:Two homogeneously charged surfaces. $C_b$=0.0005 mol/m$^3$**

After performing the first examinations on the model to see how accurate the numerical solution is in comparison with the analytical results, the model will be transformed into a 2-D box with the same dimensions by setting the other two boundaries into charged surfaces. At this step, it is assumed that the flow direction is normal to the cross section and the cross section is constant along the channel. The purpose is to see how the electric potential distribution changes in one cross section of the domain. The distribution profile of electric potential is being examined in the new transformed model, which gives the results of the 2-D model. Figure 10 shows the 2-D box model by equal dimensions and the $C_b$ concentration is equal to 0.0005 mol/m$^3$.

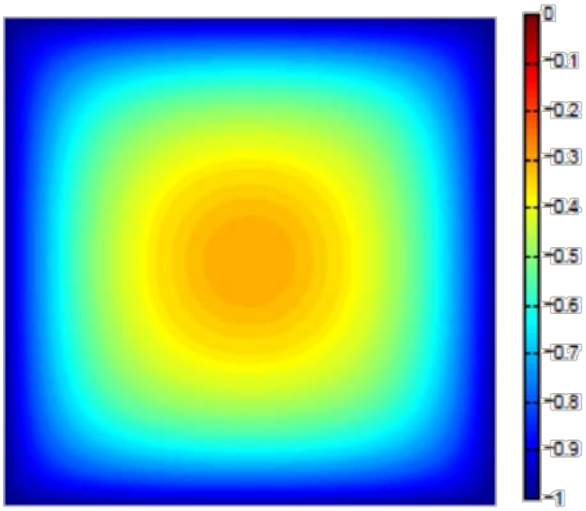


**Figure 10 : 2-D domain with homogeneously charged boundary.**

As it can be seen in Figure 10 , due to low $C_b$ concentration in the domain, again the electric potential cannot reach zero even at the center of the domain, which is because of large Debye length at low concentrations and double layer overlapping.

The reason of having a higher density of counterions near the surfaces is their mutual repulsion. However, they do not feel any attractive force between the two surfaces because the two opposing fields emanating from the two plane parallel surfaces cancel out each other in that region.

## 3.3. Three-dimensional Example

This model is a rectangular micro channel with 0.5 micrometers height, 1 micrometers width, and 2 micrometers depth, which is assumed to be carrying a Newtonian fluid. The channel has charged boundaries and the fluid enters from one side and exits from the other side. Similar to the 2-D model, the equilibrium situation is studied.

The first step in studying the 3-D domain is to set all the four surfaces to have an equal homogenous zeta potential of -1 microvolt.

This model is also solved for the heterogeneous situation, At this step, each charged surface (top, bottom, right, and left) is being divided into several partitions, each carrying a specific zeta potential. In order to have almost random charge densities in each surface, the number of these partitions must be as many as possible, which of course needs more memory to be solved.

The current model is being divided into five sections in top and bottom surface and four sections in right and left ones. Each section, as mentioned before, carries a different or

similar charge density to its neighbor sections. Figure 11 shows the 3-D electric field in this channel. The electric field is highly influenced by the boundaries. It should be noted that the Debye length is not a function of zeta potential, but the ionic concentration.

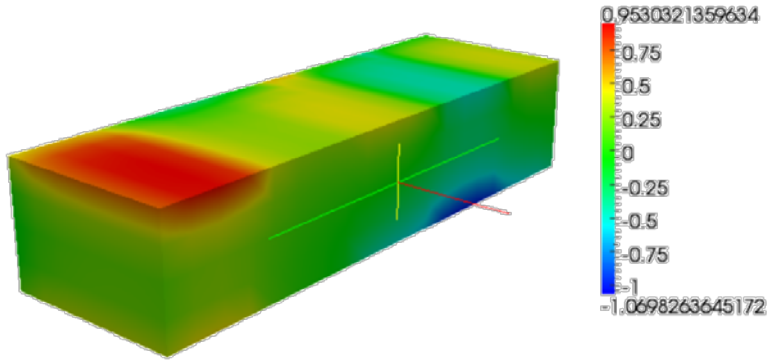


**Figure 11 : A cross-section of the electric potential distribution in a heterogeneous domain**

### 3.3.1. The effect of overlapping and aspect ratio

To analyze the effect of overlapping double layer and aspect ratio of cross section two parameters are introduced. These parameters include geometrical and physical conditions.

The first one is the ratio between the larger dimension of the domain to the smaller one (Here, the ratio of width to height). It is denoted by $\overline{W}$ and will take values of 1, 2, and 5 as is being shown in Table 1. Therefore, the first changing characteristic of the model would be its size, which starts from the equal dimensions and continues to having the width of five times larger than its height. Another is the ratio between the smaller dimension to Debye length, denoted by $\overline{K}$. This term decides if the channel is experiencing an overlapping of the double layers or not. Having a small $\overline{K}$ ratio means that the double layer has a larger length than the height of the channel, therefore, the overlapping is dominant in the domain. By having bigger amounts of this ratio, the overlapping will diminish and the electric potential tends to become zero at the mid-plane.

The effect of each of these conditions and their combination is examined and being shown in Table 1.

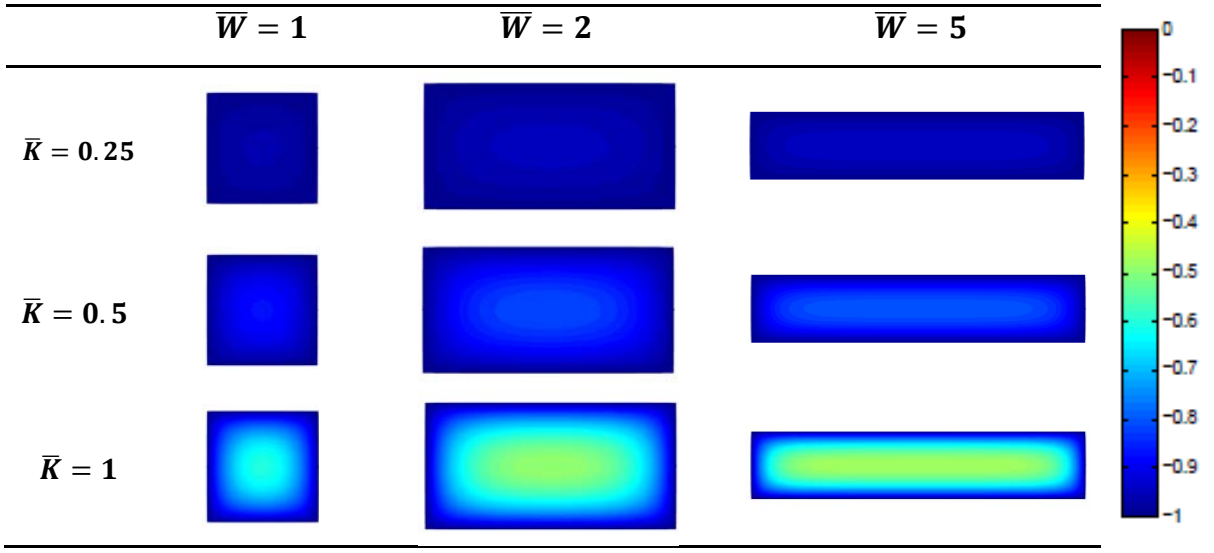


**Table 1 : Change of Electric Potential Profile in different $\overline{K}$ and $\overline{W}$ ratios**

As shown in Table 1, changing the dimension ratio in the domain makes a slight change in the electric potential distribution. For a given $\overline{W}$, making a change in the $\overline{K}$ ratio has a significant effect on the distribution profile of the electric potential and diffuse double layer. This fact shows the importance of Debye length in determining the potential distribution potential and overlapping effect in the channel.

## 3.4. An example of heterogeneously distribution of electric potential

As mentioned before, the three-dimensional model was run in two types of surface charges; Homogeneous, and heterogeneous. In the homogeneous situation, the four surfaces of the domain have the equal charge of -1 microvolts. The under study variable in order to see the behavior of the electric potential among the length of the channel is the ratio between height and Debye length, $\overline{K}$, which was also being used in the 2-D model. This ratio will be a reference for examining the double-layer overlapping situation.

For different $\overline{K}$ ratios, the model is being run in the homogeneous domain. In order to change this ratio at each step the $C_b$ concentration is changed. By changing the $C_b$, the ionic strength of the solution takes a different value, which in the end, affects the Debye length. Using this method, for having different $\overline{K}$ ratios, there would be no need to change the dimensions of the channel as it will be changed by having different Debye lengths. Figure 12 shows the cross section of the domain with $\overline{K} = 0.24$, the double-layer overlap can be seen in the cross section, as the surface zeta potential value has advanced through the mid-plane of the channel.

As it can be seen, the electric potential does not reach zero value at the mid-plane of the domain, which means that the overlapping is taking place. This phenomenon is expected, since the Debye length is almost twice as big as the height of the channel. The total results

of the homogeneous model in different $\overline{K}$ ratios are shown in Figure 13. The height of the channel is being changed to 0.3 micrometers here.

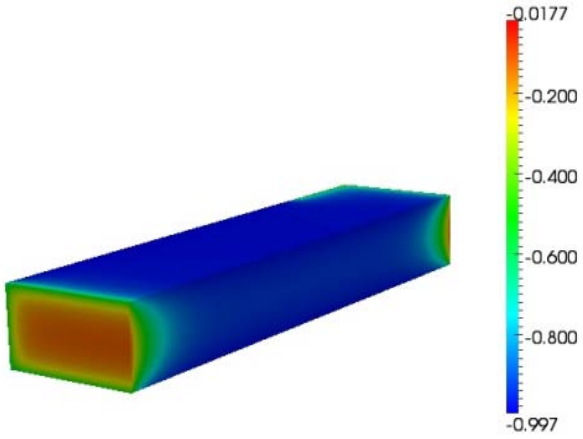


**Figure 12 : The cross section of the Homogeneous domain with overlapping diffuse double-layer**

By running the homogeneous model for several $\overline{K}$ values, the different behavior of the system from a situation in which the double layers are fully overlapping to a condition with no overlapping are plotted in Figure 13.

The five conditions are shown in Figure 13. As can be seen, the changes in the electric potential distribution are more in low $\overline{K}$ ratios. This variation in the potential profile takes place between the ends of the channel and the interior part of it zero zeta potentials at the inlet and outlet. In higher $\overline{K}$ values, this difference is much lower(the effect of boundaries become less important) , as by having smaller Debye length, the potential reaches zero close to the surface, causing the counterions stay near the walls.

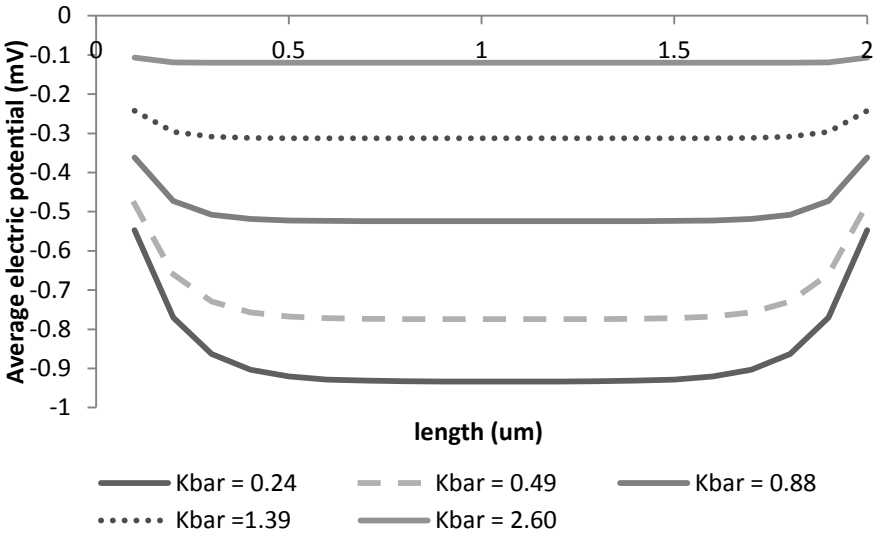


**Figure 13 : The average electric potential in length layers of the channel at different $\overline{K}$ ratios**

At lower $\overline{K}$ values, where the effect of double-layer overlapping can be seen, the electric potential does not reach zero value at the mid-plane of the channel.

In the heterogeneous model, it is assumed that the surfaces can take any potential at the surface. Therefore, a random set of potentials is being chosen for each of the surfaces. For a $\overline{K}$ ratio of 0.24, the cross section of the channel along its length is being shown in Figure 14.

As it can be seen in Figure 14, the potential distribution does not obey a specific pattern and the overlapping phenomenon of the channel cannot be predicted easily because the boundary is heterogeneous and can have even different signs for zeta potential. On the other hand, there would be the possibility of having the overlapping as a local situation instead of a global one, which is dominant through the whole channel.

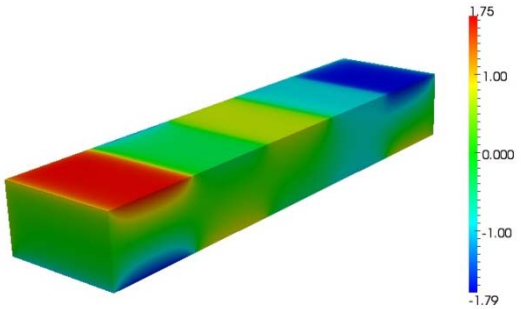


**Figure 14 : Electric field in a longitudinal cross section of a heterogeneous channel**

Although the $\bar{K}$ ratio shows that the deby length is larger than the height of the channel, but the overlapping of the diffuse double-layer cannot be seen obviously in all parts of the domain. Figure 15 shows the average electric potential change in the length layers of the channel in respect to the zeta potential value (average over the cross section).This allows us to check the overlapping of the diffuse double-layers. The overlapping is happening at the parts where the electric potential values are close to the zeta potential curve. Therefore, it can be recognized at specific parts as a local phenomenon. Basically, different signs of zeta potential at a cross section will force the electric field to be zero somewhere in the space which will dictate the $\Psi = 0$ plain (bulk concentration).

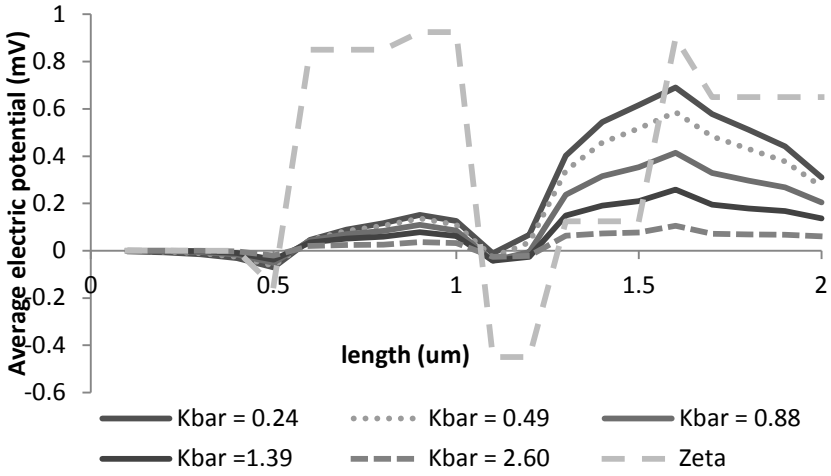


**Figure 15 : The average electric potential in length layers of the channel at different $\bar{K}$ ratios in heterogeneous domain**

## 4. Electroosmotic permeability in a single channel

Up to here, the electric field in charged microchannels using Poisson-Boltzmann distribution has been showed.

In this part, the effect of controlling parameters ($\bar{K}$ and $\bar{W}$) on the electroosmotic permeability is studied. This has been simulated using the linear Stokes flow under an external electric field.

First, linear, and non-linear Poisson-Boltzmann equations have been solved numerically for different types of boundary conditions. The simulations are run for different pH values as well.

Results can be classified into four groups:

- Linear PB equation with constant potential boundary condition.
- Non-linear PB equation with constant potential boundary condition.
- Non-linear PB equation with constant charge boundary condition.
- Non-linear PB equation with constant charge boundary condition at different. pH values.

At each step, the effects of $\bar{K}$, and $\bar{W}$ on the electroosmotic permeability are studied. Also, according to the derived results, a function has been fitted to the results. The general form of the function has been chosen so that it can match the asymptotes in extreme ranges of $\bar{K}$ and $\bar{W}$.

Here the results of these four simulation groups are presented. In all simulations, the fluid viscosity and the electric field are set to 0.001 $kgm^{-1}s^{-1}$ and 100 $Vm^{-1}$, respectively. The values of $\bar{K}$, range from 0.116162 to 116.1619. On the other hand, the dimensions of the channel are also being changed to calculate the velocity in respect to $\bar{W}$, which represents the ratio of the channel's dimensions and ranges from 1 to 20.

## 4.1. Linear PB equation with constant potential boundary condition

Solving Eq. 11 will result in the velocity field. The process of discretization is similar to the procedure, which was taken for solving the Poisson-Boltzmann equation for the electric potential; therefore, it is not being repeated again. First, the electric field is solved. Having the electric field, the velocity is solved. The variation of Keo as a function of $\overline{K}$, and $\overline{W}$is shown in Figure 16. The thick dashed line at the top of the curves represents the maximum value of electroosmotic permeability, calculated through the Smoluchowski equation.

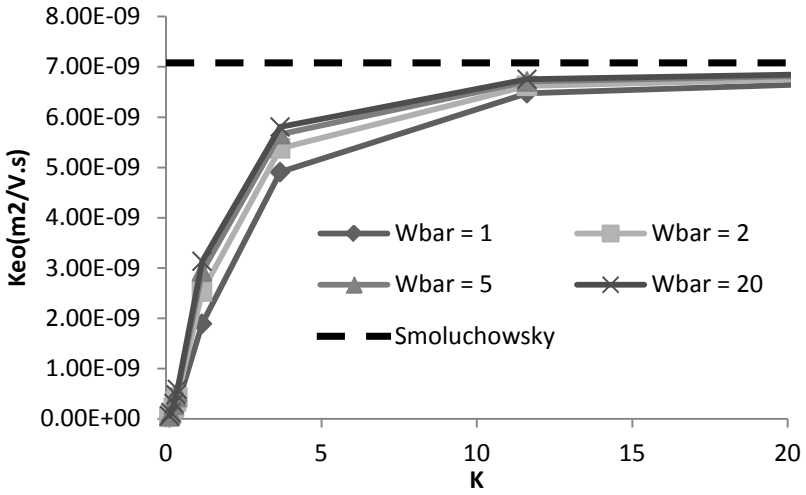


**Figure 16 : Electroosmotic permeability as a function of $\overline{K}$ and $\overline{W}$ , ξ = -10mV**

It can be seen that the Keo values reach at the highest levels to a value equal to the Smoluchowski velocity and remain constant. At high $\overline{K}$s, the Debye length thickness is at its lowest value. At this point, the electroosmotic velocity is only – and directly- dependent on the zeta potential of the channel (Kim, et al. 1996).

This is the situation, the Smoluchowski's equation is obtained as the velocity reaches its highest values and stays constant. According to Arulanandam, et al.(2000), the velocity profile follows at maximum value follows a plug-like profile, which increases from zero to a maximum level near the wall.

The unique profile of the velocity can be explained by the presence of strong electrical field near the walls, which exerts a driving force to the fluid body, which is due to excessive net charge density in EDL region (Arulanandam and Li 2000).

In contrast, when the $\overline{K}$ ratio is lower than one, EDL overlapping is taking place. This fact can happen either in case that the ionic bulk concentration is high or the height of the channel is too small compared with the EDL. At this situation, the velocity profile cannot be fully developed and does not follow a piston-like velocity profile. Thus, the electroosmotic flow does not use the whole cross-section of the channel for transporting the fluid. This means that Keo will be smaller than a fully developed velocity profile. This behavior is not in agreement with Acar et. al who concluded that the electroosmotic flux is at its highest level

when high water contents and low electrolyte concentrations are dominant, as it increases the EDL's thickness(Acar, Galeb, et al. 1995).

To illustrate the effect of overlapping double layer on velocity profile, velocity profiles for four different $\overline{K}$ values have been shown in Figure 17. It shows that velocity profile cannot be fully developed for lower $\overline{K}$ (e.g. 0.11) and the peak value of the velocity profile is much higher at higher $\overline{K}$. This is due to the fact that in higher ionic strength the imbalance of ions are denser close to the solid boundary. That creates a larger external force compared to the low ionic strength electrolytes.

Although larger $\overline{K}$ values in a single channel would result a higher fluid velocity (but not larger than the Smoluchowski velocity), at Darcy scale, the maximum volumetric flux is attained for a system where more pores do exist in a cross section to convey more fluids. Basically, at Darcy scale, there is a trade-off between the $\overline{K}$ effect and the maximum number of pores per unit cross section to provide the maximum electroosmotic permeability. If the pores were very tight so that $\overline{K}$ is very small, although there would be so many pores per unit area of the cross section, the Keo per pore would be small. On the other hand if the pores are very large, there is a limit flow rate that a single pore can transport thus the small number of pores per unit area of cross section will result a very small flux.

As a result, the increase in electroosmotic flux with increase of pore size at Darcy scale can be explained as the effect of $\overline{K}$ and decrease of electroosmotic flux with increase of pore size for larger pores can be explained by the effect of limited number of pores per cross section (limited specific surface area of the solid phase).

Another conclusion can be made by considering the situation in Figure 18. The effect of $\overline{W}$ is relatively less than effect of $\overline{K}$. As it can be seen, the profiles do not show a significant change in different $\overline{W}$ values, while in a given $\overline{W}$, Keo changes significantly. The explanation to this fact can be the independence of Debye layer of $\overline{W}$. By having higher $\overline{W}$, the only changing parameter is the width of the channel, which does not affect the EDL. Therefore, the value of electroosmotic velocity does not show a significant change.

In order to be able to apply the numerical results for upscaling purposes using pore-network modeling, the results shown in Figure 18 have been fitted to a function which has been proposed based on the general trend of the curves as follows:

$$\boldsymbol{K_{eo}} = \frac{\xi \varepsilon}{\mu} \frac{\left(1-e^{c\,\overline{W}}\right)\overline{K}^{a}}{(b+\overline{K}^{a})} \quad \textbf{Eq. 26}$$

Where

a =1.7858, b =2.1641, c =-1.5575

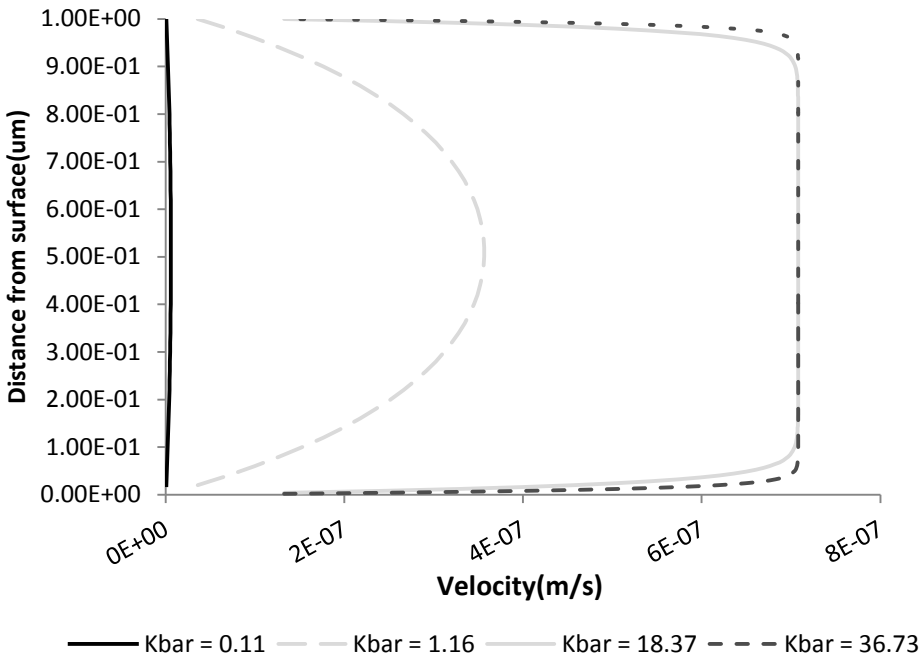


**Figure 17 : Velocity profiles at different $\overline{K}$ ratios.**

Using Eq. 26, the results for $K_{eo}$ in the pore sizes of the range 0.001 to 12 microns can be calculated. The mentioned calculations have been performed over three values of $\overline{W}$, namely, 1, 2, and 5. At each pore size, a corresponding $\overline{K}$ ratio can be calculated by dividing the pore size by Debye length. The values of $\overline{K}$ vary from the situation with EDL overlapping to the situation without overlapping by pore size and $\overline{K}$ growing.

Performing the mentioned procedure, results in a series of values for $K_{eo}$, which can represent the $K_{eo}$ distribution among the different pore size, in three $\overline{W}$ values. The results are shown in Figure 18. The results of the previous calculations is also being shown to compare the actual numeric solving results with fitting results. These results show a good match between the model and fitting.

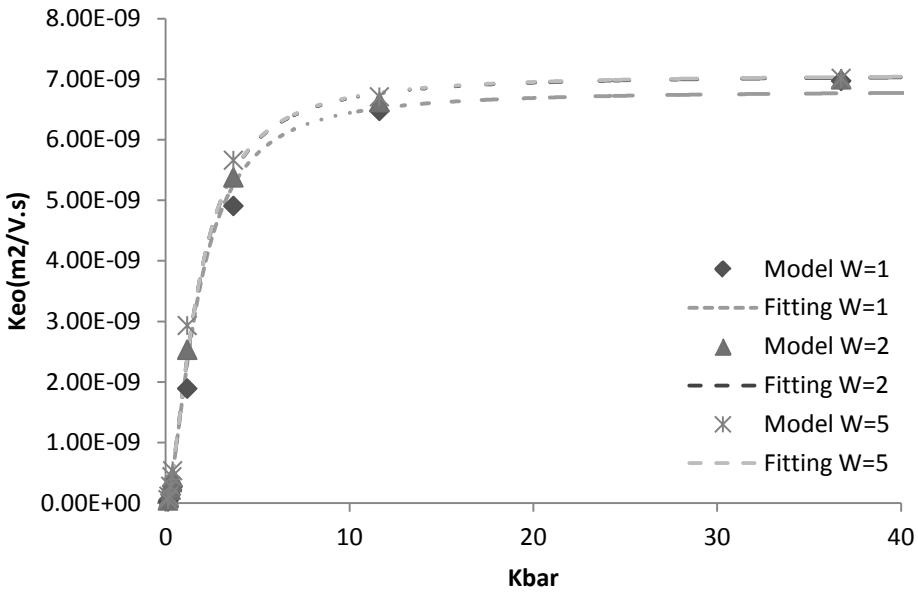


**Figure 18: $K_{eo}$ versus $\overline{K}$ for different $\overline{W}$, ξ = -10 mV**

### 4.1.1. Electroosmotic flow vs. hydrodynamic flow

As shown in Figure 19, increase of hydrodynamic permeability is much larger for larger pores due to the effect of pore geometry. However, pore size cannot influence the electroosmotic permeability as it reaches a plateau.

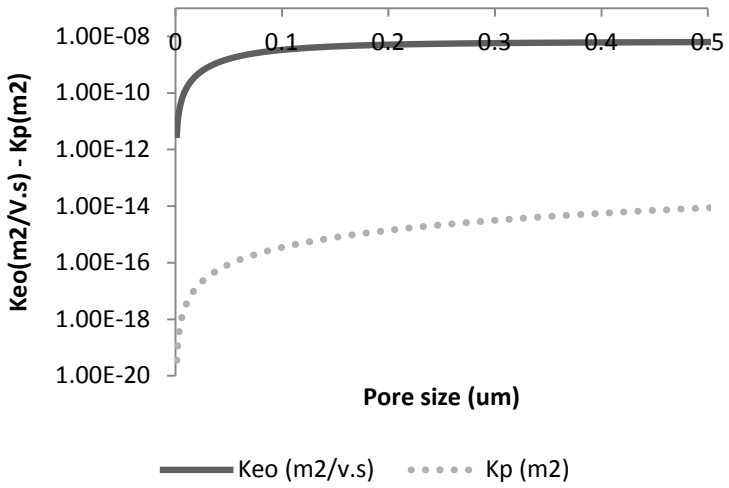


**Figure 19 : $K_{eo}$ and $K_p$ , $\overline{W} = 1$ , ξ = -10mV**

## 4.2. Non-linear PB equation with constant potential boundary

The electroosmotic permeability has been also studied using the nonlinear PB equation for different $\overline{K}$ and $\overline{W}$ values. The amount of zeta potential was set to -0.01 V similar to the linear equation. The ranges of $\overline{K}$ and $\overline{W}$ were the same as the previous section.

The results were fitted using the same general form as the linear PB fitting function. However, as the values of Keo, in non-linear equation were different from the linear results, the parameters of the fitting equation were calculated again as follows:

a =1.7112 , b =2.2073, c =-3.2129

Having the results of model and fitting equation, the variation of the electroosmotic permeability versus $\overline{K}$ is showed in Figure 20.

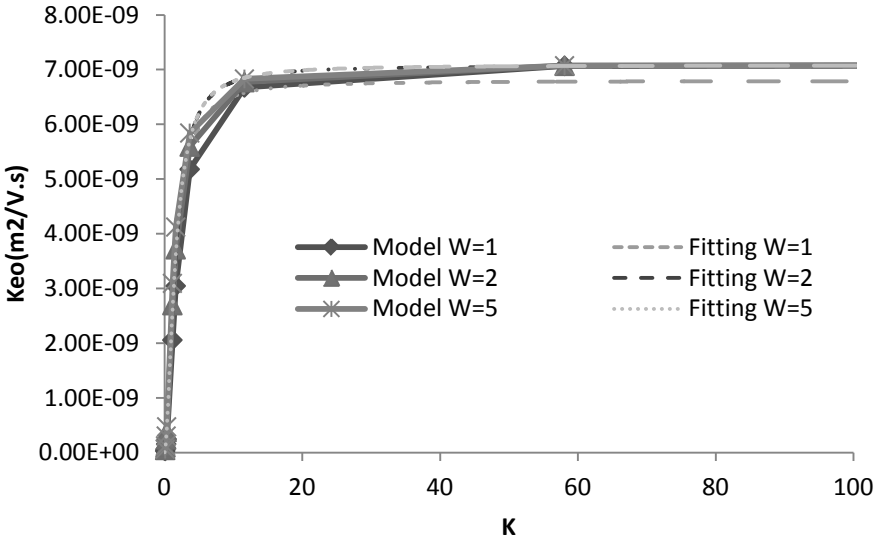


**Figure 20: Electroosmotic permeability in different $\overline{K}$ and $\overline{W}$, for the nonlinear PB equation under constant potential of -10mV**

As expected the trend of the Keo does not seem a major difference between the linear and non-linear models for small zeta potential as the linearization of PB is valid.

### 4.2.1. Comparing the results of linear and non-linear models

The trend of the electroosmotic permeability is not different in linear and non-linear models, as both equations result in a increase of electroosmotic permeability from lower values in small $\overline{K}$, up to the maximum value of Smoluchowsky Keo. However, the magnitude of Keo has been different. As shown in Figure 21, for zeta potential value of -10 mV, the linear model shows relatively higher values than the non-linear model. This can be explained through the fact that in non-linear equation, using the proper $\boldsymbol{Sinh}\left(\frac{e\,Z_i\,\Psi}{k_B\,T}\right)$ in PB equation, the value of potential will decay faster to reach the neutral plane. Therefore, velocity profile would develop better for given material and geometrical parameters under nonlinear PB.

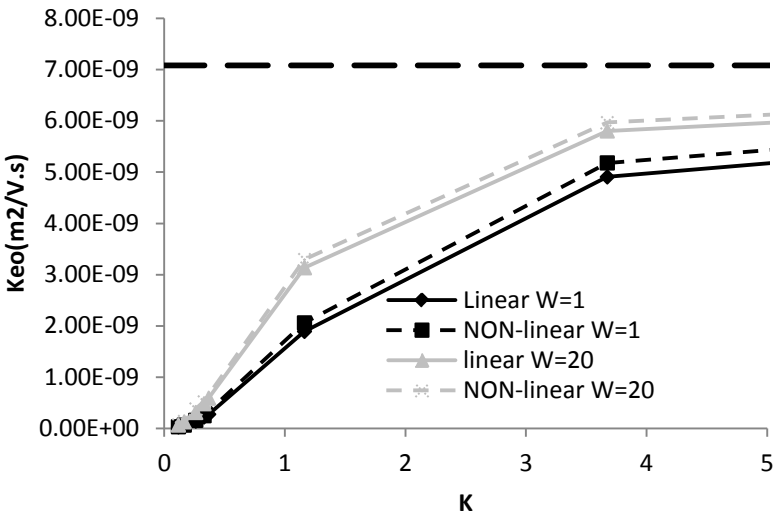


**Figure 21 : Electroosmotic permeability profiles, linear vs. non-linear model, ξ= -10mV**

## 4.3. Non-linear PB equation with constant charge boundary

For a constant charge boundary condition, the linear PB cannot be used as its results would be unrealistic. At this section, the non-linear Poisson-Boltzmann equation is being solved numerically Since, the boundary conditions are set to constant charge, the surface potential would change for different geometrical and physically parameters. The new boundary condition has been solved in surface charge equal to 0.2 $Cm^{-2}$. The model is solved for several bulk concentrations, $\overline{K}$ ratio, and $\overline{W}$ ratio.

$\overline{K}$ ratio depends on the ionic concentration and takes values related to that. $\overline{K}$ values was set for five values. $\overline{W}$ was set to 1, 2, and 5. For each value of the surface charge, fifteen different conditions were calculated. The results show how the electric potential varies with respect to the geometric factors. The results are shown in Figure 22. It can be seen that the trend of electroosmotic permeability is the same as the previous conditions, as expected. However, at lower $\overline{K}$, the changes are not as steep as in the previous sections. The difference between the Keo values in different $\overline{W}$ ratios, is almost zero, which implies the low effect of this parameter on electroosmosis. All of the curves reach at high $\overline{K}$ to the maximum value of Smoluchowski, which cannot be calculated analytically at this section, as the zeta potential value is not known. The value of Smoluchowski Keo was derived from the results directly.

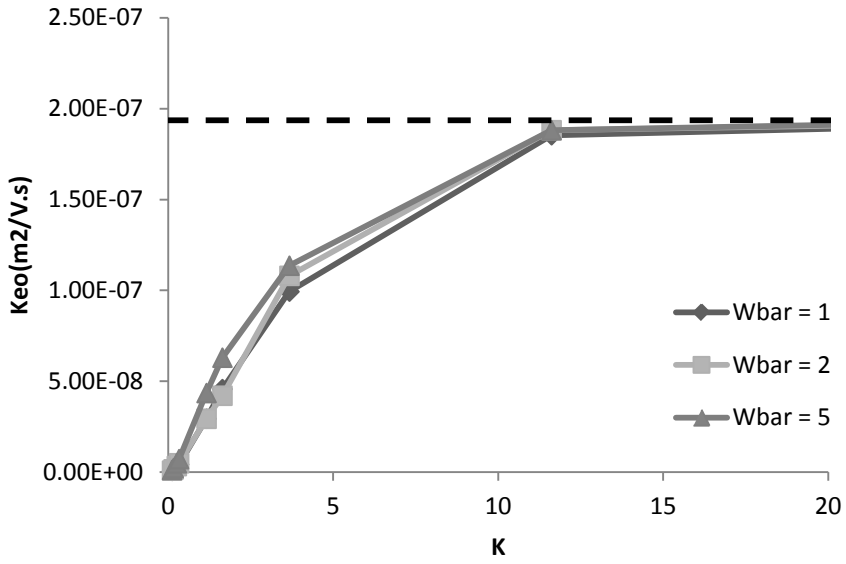


**Figure 22 : The distribution profile of electroosmotic permeability, non-linear PB with constant charge, $\sigma = 0.2\ C.m^{-2}$**

The model results were also being used to create the fitting function for electroosmotic permeability values. The fitting results are compared to the model results in Figure 23. As the different profiles of Keo were at similar values for different $\bar{W}$s, only $\bar{W} = 1$ was used to show the model and fitting results.

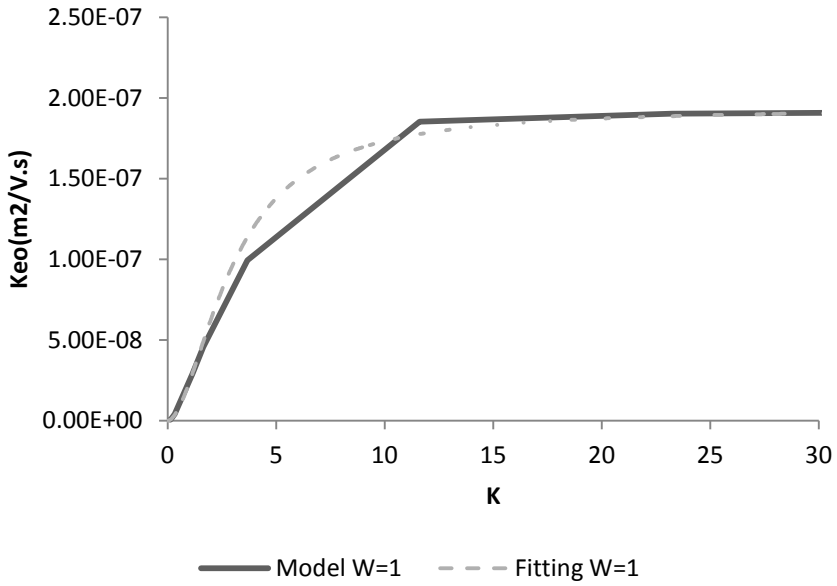


**Figure 23 : Electroosmotic permeability in different $\bar{K}$, $\sigma = 0.2\ C.m^{-2}$**

### 4.3.1. Electroosmotic flow vs. hydrodynamic flow in non-linear PB equation

The electroosmotic permeability was compared to the hydrodynamic permeability in the non-linear PB model with the constant charge boundary condition.

The results are shown in Figure 24. The vertical axis is the permeability (Kp and Keo) in logarithmic scale.

As seen, the behaviour of the model is the same as in the linear model. Although the ranges of values differ and Keo in constant charge boundary condition reaches larger values.

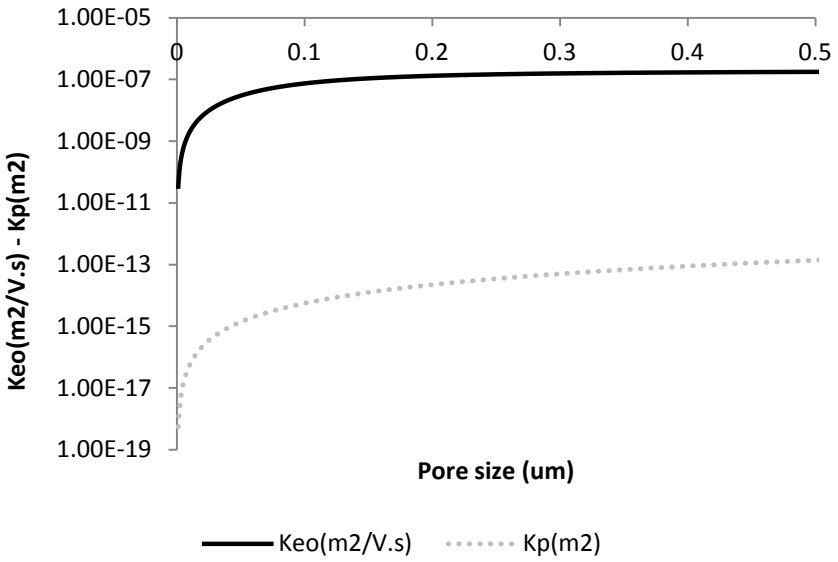


**Figure 24 : Comparison between electroosmotic and hydrodynamic permeability in non-linear PB model using constant charge boundary condition. $\sigma = 0.2\ C.m^{-2}$**

## 4.4. pH effects on electric field and electroosmotic permeability for a constant charge boundary condition

Based on the constant charge boundary condition and including pH effects on active charge (Eq. 17), the nonlinear Poisson-Boltzmann equation (Eq. 4) has been solved and the electroosmotic permeability has been calculated.

The results have been shown for different pH value, $\overline{K}$, and $\overline{W}$ values.. According to the proposed chemical reactions in (Eq. 17), the pH variations affect the ionic interactions between the channel wall and the electrolyte fluid. Eq. 17 explains directly how these interactions are related to the concentration of the proton and sodium ions. The ionic interactions at the next step determine the variations in surface charge density, which itself has a direct relation with the gradient of potential normal to the surface according to Eq 18.

The pH effects are being studied for the values of pH=3, 5, 6, 7, 8.

Figure 25, shows the results. In small $\overline{K}$values, the system is experiencing strong overlapping double layer.

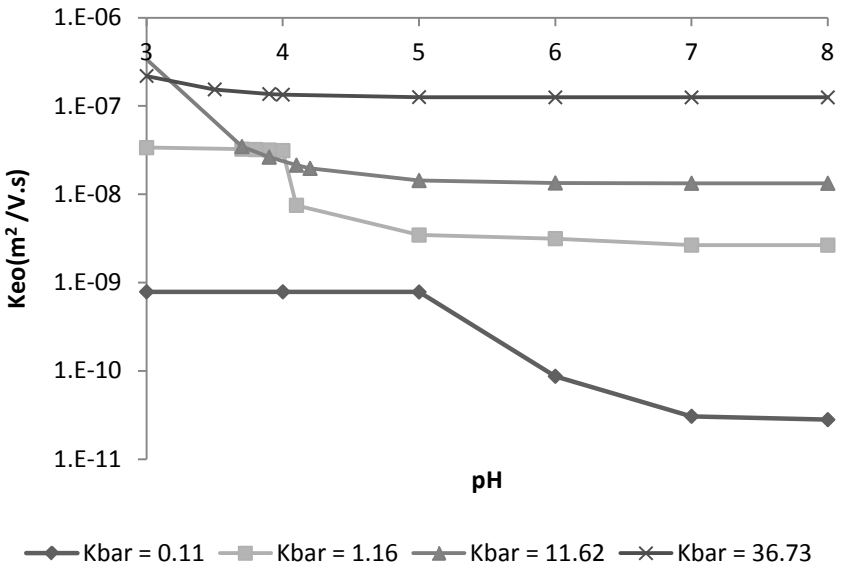


**Figure 25 : The profile of Keo as a function of pH, and $\bar{K}$ ratio for $\bar{W} = 1$ . $\sigma_{max} = 0.7\ C.m^{-2}$**

Vertical axis represents the logarithmic values of Electroosmotic permeability. As seen in Figure 25, for a given pH value, $K_{eo}$ is the smallest for the smallest$\bar{K}$. This has the same trend as the Keo as a function of $\bar{K}$ in previous simulations.

All the profiles experience a decline by increase of pH values. The decline of Keo at higher pH values is a result of decline of availability of proton ions to interact with the charged surface. As a result the interaction with sodium ions will increase that would influence the electric field to have larger penetration length scale and consequently smaller electroosmotic permeability. There is good agreement between this result and literature data. According to experiment data from Beddiar, et, al (2005), increasing pH values result in decrease in the magnitude of electroosmotic permeability. Same experimental results were observed with Lorenz(1969). Also experimental data by Leland, et al., (1997), and Kim, et al., (1996) showed that increasing pH results in having less negative zeta potentials, considering the direct effect of zeta potential on the electroosmotic permeability, the same result can be concluded.

As it can be seen, for smaller $\bar{K}$ values this effect is stronger as the whole cross section of the channel is under influence of an electric field.

To show the effect of$\bar{W}$, the Keo values versus pH for different $\bar{W}$have been plotted in Figure 26. $\bar{K}$ in this graph is set to 0.58. As it shows, the effect of $\bar{W}$ cannot be as important as $\bar{K}$ similar to the results for constant potential conditions.

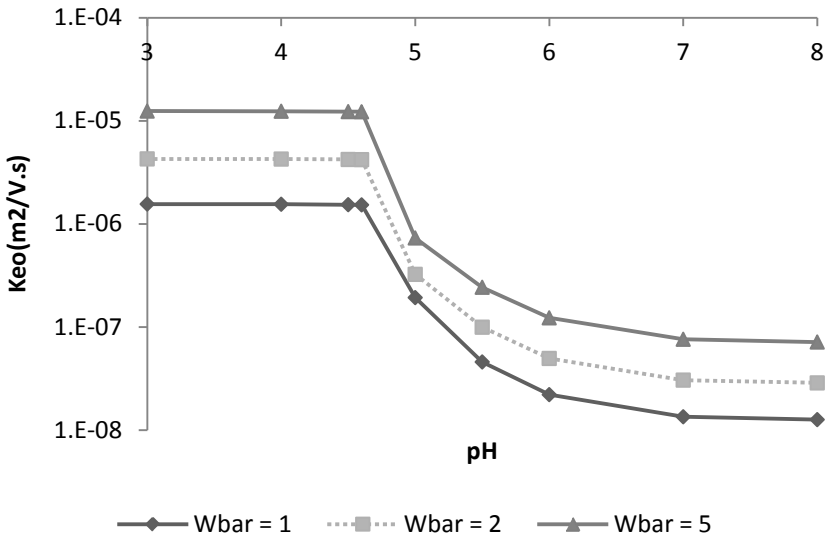


**Figure 26 : Keo profiles for different $\overline{W}$ values under pH effect, $\overline{K}$=0.58**

The pattern of declining of different profiles in the latter figure is also uniform, while the different profiles in the former take different declining points.

# 5. Conclusion

The Poisson-Boltzmann equation was solved numerically in two forms of linear and non-linear in a microchannel. The electric potential was calculated in two and three-dimensional forms, where the domain was assumed to be a cross section of a microchannel, normal to the flow direction, and the whole channel, respectively. The results in one dimension were compared to the analytical solution of the PB equation, by assuming the domain as consisting of two parallel charged plates. There is rather a small difference between the analytical and numerical model especially for overlapping condition which can be due to the linear PB solver..

To calculate the electroosmotic permeability, first the potential was solved by the PB equation (linear and nonlinear forms). Then, the velocity profile of the channel was calculated through stokes equation. Four different situations were considered in the numerical solution;

- Linear PB equation with constant potential boundary condition.
- Non-linear PB equation with constant potential boundary condition.
- Non-linear PB equation with constant charge boundary condition.
- Non-linear PB equation with constant charge boundary condition at different. pH values.

At each part the effects of influencing factors (scaling between the Debye length and half of the channel height and the aspect ratio of the channel) on electroosmotic permeability were investigated. The results were compared between the linear and non-linear equations with constant potential boundary condition. At both models, it could be concluded that the effect of $\overline{K}$, the ratio of height of the channel to the Debye length was crucial, while $\overline{W}$, the aspect ratio had a minor effect on the electroosmotic permeability, compared to the other factor. The results of each solution were fitted using a general form of an empirical relation that fits well with the data.

The electroosmotic permeability was compared to the hydrodynamic permeability at each step. This comparison was made in order to determine the different conditions, where each

of the methods can be effective. This fact determines the effectiveness of EOF in fine pores, the base of EOF application in a wide range of industrial cases, (e.g. soil remediation).

In addition, a comparison between the results of non-linear equations at different boundary conditions was performed. At this step, although the values of Keo were different, however, the electroosmotic permeability profiles followed same distribution profile patterns.

The pH effects were also investigated in terms of their influence on the electroosmotic permeability. It was observed that the magnitude of Keo declines as the pH increases. Such behavior of the electroosmotic permeability was explained through the fact that at higher pH, as the amount of proton ions becomes fewer, the reactive sites of the surface will be more neutralized with the electrolyte's dissociated cations. This fact leads to a decrease in the potential effects on the fluid, and as a result, the flow rate declines.

An important result was the behavior of the electroosmotic permeability in different $\overline{K}$values. The profile started at low magnitude and increased as the $\overline{K}$increased from small values, which denoted the overlapping of EDLs to large values, with no overlapping. The highest magnitude of Keo was found to be at a value, which could be calculated through the Smoluchowski equation and remained constant. The comparison between the velocity profiles of different $\overline{K}$s indicated that at low EDL thicknesses the magnitude of the velocity profile reaches at this maximum value due to presence of high net charge density close to the surface of the channel. This fact was dominant at all the above-mentioned states of solving the PB equation.

# 6. References

Acar, Yalcin.B, and Akram.N Alshawabkeh. "Principles of Electrokinetic remediation." *Environmental science & technology*, 1993.

Acar, Yalcin.B, et al. "Electrokinetic remediation: Basics and technology status." *Journal of Hazardous Materials* (Elsevier), 1995.

Afonso, A.M., F.T. Pinho, and M.A. Alves. "Electro-osmosis of viscoelastic fluids and prediction of electro-elastic flow instabilities in a cross slot using a finite-volume method." *Journal of Non-Newtonian Fluid Mechanics* (Elsevier), 2012.

Ajaev, Vladimir S. "Chapter 4 : Flows in the Presence of Electric Charges and Fields." In *Interfacial Fluid Mechanics, A Mathematical Modeling Approach*, 101-124. 2012.

Ajdari, Armand. "Electro-Osmosis on Inhomogeneously Charged Surfaces." (PH YS ICAL REVIEW LETTERS, VOLUME 75, NUMBER 4) 1995.

Arulanandam, Sarah, and Dongqing Li. "Liquid transport in rectangular microchannels by electroosmosis pumping." *Colliods and Surfaces*, 2000.

Bowen, W. Richard, and Robert A. Clark. "Electro-osmosis at Microporous Membranes and the Determination of Zeta-Potential." *Journal of Colloid and Inte(face Science* (Academic Press, Inc.) 97 (1983).

C. Prievet, Dennis, and Eli Ruckenstein. "The Surface Potential of and Double-layer Interaction Force between Surfaces characterized by Multiple Ionizable Groups." *J. theor. Biol*, 1976.

Chen, Jiann-Long, P.E. M.ASCE, Souhail Al-Abed, James Ryan, Mike Roulier, and Mark Kemper. "Effects of Electroosmosis on Soil Temperature and Hydraulic Head. II: Numerical Simulation." *Journal of Geotechnical and Geoenvironmental Engineering*, 2002.

Coelho, D, M Shapiro, J.F Thovert, and P.M Adler. "Electroosmotic Phenomena in Porous Media." *JOURNAL OF COLLOID AND INTERFACE SCIENCE* 181 (1996): 169–190.

Corapcioglu, M.Yavuz. "Formulation of Electro-Chemico-Osmotic Processes in Soils." *Transport in Porous Media* (Kluwer Academic Publishers), 1991.

Herr, A.E., J.I. Molho, J.G. Santiago, M.G. Mungal, and T.W Kenny. "Electroosmotic Capillary Flow with Nonuniform Zeta Potential." *Analytical Chemistry* (American Chemical Society), 2000.

Israelachvili, Jacob N. *Intermolecular and Surface Forces.* 3. 2011.

Joekar Niasar, Vahid, Ruud Schotting, and Anton Leijnse. "Analytical Solution of Electro-Hydrodynamic Flow and Transport in Rectangular Channels: Inclusion of Double Layer Effects." *Computational Geoscience* (Springer), 2013.

JORGENSON, JAMES W., and KRYNN DeARMAN LUKACS. "HIGH-RESOLUTION SEPARATIONS BASED ON ELECTROPHORESIS AND ELECTROOSMOSIS." *Journal of Chotnafography* (Elsevier), 1981.

Kang, Yuejun, Chun Yang, and Xiaoyang Huang. "Analysis of the Electroosmotic flow in a microchannel packed with homogeneous microspheres under electrokinetic wall effects." *International Journal of Engineering Science* (Elsevier), 2004.

Kim, K.J., A.G. Fane, M. Nystrom, A. Pihlajamaki, W.R. Bowen, and H. Mukhtar. "Evaluation of electroosmosis and streaming potential for measurement of electric charges of polymeric membranes." *Journal of Membrane Science* (Elsevier) 116 (1996).

Kim, Seong-Hye, Hyo-Yeol Han, You-Jin Lee, Chul Woong Kim, and Ji-Won Yang. "Effect of electrokinetic remediation on indigenous microbial activity and community within diesel contaminated soil." *Science of the Total Environment* (Elsevier), 2010.

Kirby, Brian. *Micro- and Nanoscale Fluid Mechanics, Transport in Microfluidic Devices.* 2010.

Leland, M.Vane, and M.Zang Gwen. "Effect of aqueous phase properties on clay particle zeta potential and Electroosmotic permeability: Implications for electrokinetic soil remediation processes." *Journal of Hazardous Materials* (Elsevier), 1997.

Lemaire, Thibault, Christian Moyne, and Didier Stemmelen. "Modelling of electroosmosis in clayey materials including PH effects." *Physics and Chemistry of the Earth 32*, 2007.

McBRIDE, MURRAY B. "A CRITIQUE OF DIFFUSE DOUBLE LAYER MODELS APPLIED TO COLLOID AND SURFACE CHEMISTRY." *Clays and Clay Minerals* (The Clay Minerals Society) 45 (1997).

Nerine, J. Cherepy, and Dorthe Wildenschild. "Electrolyte Management for effective Long-term Electroosmotic transport in low permeability soils." *Environmental Science and Technology* (American Chemical Society), 2003.

O'BRIEN, R. W. "Electroosmosis in Porous Materials." *Journal of Colloid and Interface Science* (Academic Press) Vol. 110 (1985).

Talapatra, Siddharth, and Suman Chakraborty. "Double layer overlap in ac electroosmosis." *European Journal of Mechanics B/Fluids* (Elsevier) 27 (2007).

Tsuda, Takao, Masakazu Ikedo, Glenn Jones, Rajeev Dadoo, and Richard N. Zare. "Observation of flow profiles in electroosmosis in a rectangular capillary." (Journal of Chromatography, 632 (1993) 201-207, Elsevier Science Publishers B.V., Amsterdam) 1993.

Wang, Moran, and Shiyi Chen. "Electroosmosis in homogeneously charged micro- and nanoscale random porous media." *Journal of Colloid and Interface Science* (Elsevier) 314 (2007).

Wang, Moran, Ning Pan, Jinku Wang, and Shiyi Chen. "Lattice Poisson-Boltzmann Simulations of Electroosmotic Flows in Charged Anisotropic Porous Media." *Cummunications in Computational Physics*, 2007.